Spontaneous Loss of Heterozygosity in Diploid *Saccharomyces cerevisiae* Cells

Mina Hiraoka,*,[1] Kei-ichi Watanabe,*,[1] Keiko Umezu*,[†] and Hisaji Maki*

*Department of Molecular Biology, Graduate School of Biological Sciences, Nara Institute of Science and Technology, Ikoma, Nara 630-0101, Japan and [†]PREST, Japan Science and Technology Corporation, Kawaguchi, Saitama 332-0012, Japan

ABSTRACT

To obtain a broad perspective of the events leading to spontaneous loss of heterozygosity (LOH), we have characterized the genetic alterations that functionally inactivated the *URA3* marker hemizygously or heterozygously situated either on chromosome *III* or chromosome *V* in diploid *Saccharomyces cerevisiae* cells. Analysis of chromosome structure in a large number of LOH clones by pulsed-field gel electrophoresis and PCR showed that chromosome loss, allelic recombination, and chromosome aberration were the major classes of genetic alterations leading to LOH. The frequencies of chromosome loss and chromosome aberration were significantly affected when the marker was located in different chromosomes, suggesting that chromosome-specific elements may affect the processes that led to these alterations. Aberrant-sized chromosomes were detected readily in ∼8% of LOH events when the *URA3* marker was placed in chromosome *III*. Molecular mechanisms underlying the chromosome aberrations were further investigated by studying the fate of two other genetic markers on chromosome *III*. Chromosome aberration caused by intrachromosomal rearrangements was predominantly due to a deletion between the *MAT* and *HMR* loci that occurred at a frequency of 3.1×10^{-6}. Another type of chromosome aberration, which occurred at a frequency slightly higher than that of the intrachromosomal deletion, appeared to be caused by interchromosomal rearrangement, including unequal crossing over between homologous chromatids and translocation with another chromosome.

GENETIC alterations leading to phenotypic changes in diploid cells are more complex than those occurring in haploid cells. Except in the case of dominant mutations, cells carrying functionally normal alleles on both homologous chromosomes usually require two genetic events, wherein both alleles are altered, to obtain a phenotypic change. For example, the first event might be a point mutation resulting in a heterozygous state with a recessive mutant allele and an unchanged normal one, while the second event could be any genetic alteration that functionally inactivates the remaining normal allele. The latter event leads to phenotypic expression of the recessive allele and is referred to as loss of heterozygosity (LOH). As proposed by the two-hit hypothesis (KNUDSON 1993) and as shown by extensive studies with familial cancers (LASKO *et al.* 1991), in most malignant cells, tumor-suppressor genes have been functionally inactivated by such mutational processes. Thus, determining the mechanisms leading to LOH is crucial in helping to understand the generation and progression of cancer as well as other diseases caused by somatic mutations.

The process of LOH can be caused not only by intra-

genic mutations but also by various genetic alterations unique to diploid somatic cells, namely, chromosome loss with or without reduplication, gross rearrangement of chromosomes, and mitotic recombination between alleles (TISCHFIELD 1997; LENGAUER *et al.* 1998). The LOH of tumor-suppressor genes in malignant cells is predominantly associated with such chromosomal alterations and allelic recombination. Different types of multiple chromosome rearrangements, such as gene amplifications, large deletions, and translocations, are often found in various kinds of cancer cells and some of the loci affected by the rearrangement correspond to tumor-suppressor genes. Despite their impact on carcinogenesis, however, molecular mechanisms underlying the genomic rearrangements are not well understood. This is due mainly to difficulties in identification and examination of the spontaneous rearrangements that occur in normal cells during mitotic division. Although aberrant chromosomes have been found in studies of spontaneous LOH in human T cells and mouse primary fibroblast cells, it has been difficult to determine the endpoints of the chromosome rearrangements because of the large size of the mammalian genomes (GUPTA *et al.* 1997; TISCHFIELD 1997). Thus, the structural constituents involved in the chromosome aberrations are not well defined. Another reason for the difficulties associated with the study of mammalian systems is that the state of local and general DNA transactions, such as replication, repair, recombination, and transcription,

Corresponding author: Keiko Umezu, Department of Molecular Biology, Graduate School of Biological Sciences, Nara Institute of Science and Technology, Takayama 8916-5, Ikoma, Nara 630-0101, Japan. E-mail: umezu@bs.aist-nara.ac.jp

[1] These authors contributed equally to this work.

vary widely between cell types. LOH is the net result of such DNA transactions and the underlying mechanisms may vary significantly among different types of mammalian cells. Because of these issues, it is advantageous to study mechanisms leading to LOH in the yeast *Saccharomyces cerevisiae*, since its genome is small and its life cycle is simple. In addition, it may be relatively easy to examine the LOH mechanisms in yeast with the availability of elaborate genetic techniques for its study and the significant amount of information about the physical and functional structure of the whole genome of the organism. Furthermore, mechanisms involved in the DNA transactions have been well documented in yeast cells as a model organism of eukaryotic systems.

LOH in yeast has been studied by examining mitotic segregation of a given genetic marker, heterozygously situated in diploid strains or in hyperhaploid strains disomic for a certain chromosome (Campbell *et al.* 1975; Malone *et al.* 1980; Esposito *et al.* 1982; Hartwell and Smith 1985; Surosky and Tye 1985; Meeks-Wagner and Hartwell 1986; Kupiec and Petes 1988; Bruschi *et al.* 1995). Although there were some differences between experiments with different genetic markers, these studies have shown that, in general, LOH in yeast cells is due mainly to mitotic recombination between alleles. In contrast with what was seen for mammalian cells, chromosome loss was the major chromosome aberration observed in the yeast LOH clones, and aberrant chromosomes were rarely found associated with LOH. Some of these differences between yeast and mammalian cells may be due to intrinsic differences between the organisms. However, it is also probable that various DNA elements spread over chromosomes affect the way LOH is generated differently. In other words, it is hard to rule out the possibility that the loci previously utilized for the yeast and mammalian studies may undergo LOH in a biased manner due to their surrounding sequences. In addition, yeast LOH that resulted from chromosome rearrangement might have been overlooked in previous studies, because LOH in yeast was analyzed primarily by genetic techniques rather than by direct examination of chromosome structures.

Studies of genetic rearrangements in yeast cells have been carried out, in the main, using haploid cells or cells in meiosis, since genetic techniques for detection of rearrangements are more applicable to haploid cells. It has been shown that spontaneous genetic rearrangements in the yeast genome occur at a detectable level between repeated sequences, such as retrotransposable elements *Ty*, the ribosomal DNA array, multiple repeats of *CUP1*, and artificially inserted duplications (Liebman *et al.* 1979; Rothstein 1979; Roeder and Fink 1982; Winston *et al.* 1984; Downs *et al.* 1985; Christman *et al.* 1988; Kupiec and Petes 1988; Boeke 1991; Keil and McWilliams 1993; Klein 1995). Recently, Chen and Kolodner (Chen *et al.* 1998; Chen and Kolodner 1999)

showed that microhomology-mediated and non-homology-mediated gross rearrangements were significantly increased in strains defective in *RFA1*, *RAD27*, *MRE11*, *XRS2*, or *RAD50* genes. These observations suggest that several different pathways of DNA recombination are involved in the spontaneous rearrangements of the genome. Some require relatively long homologous DNA sequences at the endpoints, and others do not require such homology. Furthermore, it seems likely that recombinogenic damage arises frequently in the genome of normal dividing cells and promotes genetic rearrangements as the consequences of errors in the recombination processes. Nevertheless, only a limited portion of genetic rearrangements can be detected when haploid cells are used, as rearrangements leading to the loss of an essential gene or DNA segment go unrecognized.

Our ultimate goal is to determine the breakpoints of aberrant chromosomes and identify chromosomal elements and particular nucleotide sequences that participate in the chromosome aberration, so as to elucidate the molecular mechanisms involved in genetic rearrangement. To reveal those structural features of chromosomes involved in genetic rearrangement, especially in the context of various DNA transactions during mitotic growth, it is important to collect a variety of aberrant chromosomes occurring within a natural diploid genome without any bias toward particular types of genetic rearrangement. To achieve this, we analyzed genetic alterations that functionally inactivated a *URA3* gene hemizygously or heterozygously situated at particular loci in diploid yeast cells, with the assumption that genetic rearrangement would be less detrimental in diploid cells compared to haploid cells. By directly analyzing chromosomes in LOH$^+$ clones by pulsed-field gel electrophoresis (PFGE) and polymerase chain reaction (PCR), we could identify several kinds of genetic alterations participating in LOH. These alterations were chromosome loss, allelic recombination, and, in particular, gross rearrangement of chromosomes. The latter had previously never been systematically examined as an event causing LOH in yeast. The chromosome rearrangements were further investigated by coupling PFGE analysis with a conventional genetic analysis. This approach allowed us to classify the chromosome rearrangements into two classes: one caused by intrachromosomal deletion and the other by interchromosomal rearrangement. In addition, the relative frequencies of the distinct LOH events were estimated and compared between the same heterozygous marker located at either of two different chromosomes.

MATERIALS AND METHODS

Media: Media for yeast strains including complex glucose (YPD), sporulation, synthetic complete (SC), and various drop-out media were made as described (Rose *et al.* 1990). The pH of SC and drop-out plates was adjusted to 7 before

autoclaving. In YPAD medium, adenine sulfate was added to YPD to 0.004%. Uracil was added to YPD and YPAD to 20 μg/ml when indicated. 5-Fluoro-orotic acid (5-FOA) plates were prepared as described (ROSE *et al.* 1990). *Escherichia coli* cells were grown in Luria broth medium (MILLER 1972) supplemented with 100 μg/ml ampicillin or 40 μg/ml each of 5-bromo-4-chloro-3-indolyl-β-D-galactoside and isopropylthio-β-D-galactoside when required (SAMBROOK *et al.* 1989). SOC medium (SAMBROOK *et al.* 1989) was used for incubation of the cells after electrotransformation.

Genetic and nucleic acid techniques: Standard methods for yeast genetics were followed (ROSE *et al.* 1990; AUSUBEL *et al.* 1994). Yeast transformations were performed using lithium acetate (GIETZ *et al.* 1992). *E. coli* transformation was carried out by electroporation using Gene Pulser (Bio-Rad, Hercules, CA) as recommended by the supplier. Restriction enzymes, T4 ligase, alkaline phosphatase, and Klenow fragment were purchased from Toyobo or Takara and used according to manufacturer's specifications. Yeast genomic DNA was isolated by a glass bead lysis method (AUSUBEL *et al.* 1994). Purification of DNA from agarose gel or DNA plugs was performed using QIAquick gel extraction kit (QIAGEN, Hilden, Germany). Plasmid DNA was isolated from *E. coli* by an alkali-lysis method (SAMBROOK *et al.* 1989) except for that used as PCR template, which was prepared with the QIAGEN Plasmid Midi kit. PCR products were purified with QIAquick PCR purification kit (QIAGEN) when used as probes for Southern hybridization. General DNA manipulations were performed as described (SAMBROOK *et al.* 1989). To quantify DNA in ethidium bromide-stained gels, the gels were photographed using a CCD video camera (Atto, Tokyo) with DensitoGRAPH software (Atto) and the intensities of DNA bands were quantified against standard DNA with Image 1.47 software (Wayne Rasband, National Institutes of Health).

***S. cerevisiae* and *E. coli* strains:** All yeast strains used were derivatives of the S288c parental strains, FY838 and FY23, kindly provided by Dr. Fred Winston (Harvard Medical School) and are listed in Table 1. Strains YKU1 and YKU21 were isolated as spore clones from the diploid constructed by the cross between FY838 and FY23. Strain YMH1 is similar to YKU1 but has the *URA3* insert at about 204,900 nucleotides on chromosome *III* [designated here as *III*-205 locus: nucleotide coordinates are given in the Saccharomyces Genome Database (SGD; http://genome-www.stanford.edu/Saccharomyces)] and was constructed by transforming YKU1 with the *Xba*I-*Xma*I *URA3* fragment of pMH116 (see below). Strain YMH5, in which *ura3-52* was replaced with wild-type *URA3*, was obtained in a similar way. Strain YMJ1 was constructed in a similar way to YMH1 except FY838 was used for the transformation instead of YKU1. Strain YMJ2 was obtained by transforming YMJ1 with the *Eco*RI fragment of pMJ118 containing *ura3-91* (see below) and selecting for 5-FOA resistant (5-FOA^r) transformants. For strain YMJ4, the *Nde*I-*Stu*I fragment of pMJ118 was used to introduce the *ura3-91* at the *URA3* locus of YKU21. YKU23 is the same as FY838 except for the presence of *ade2Δ::hisG*, which was made by the method using the *hisG-URA3-hisG* construct as described (ALANI *et al.* 1987). The *ADE2* disruption fragment was constructed by PCR and was composed of three parts, the first 60 bp of the *ADE2* open reading frame (ORF), the *hisG-URA3-hisG* region of plasmid pNKY51 (ALANI *et al.* 1987), followed by the last 60 bp of the *ADE2* ORF. The primers used were dAFh505 and dARh2214 (Table 2). YKU34 is the same as YMH1 except for the presence of *ade2Δ::hisG* and two markers on chromosome *III*, *LEU2* and the *ADE2* insert at about 314,000 (designated as *III*-314 locus) in addition to *III*-205::*URA3*. YKU34 was constructed by the following steps: YKU1 was converted to *ade2Δ::hisG* as for YKU23. The *URA3* insertion was as described for YMH1. *leu2Δ1* was

transplaced to *LEU2* with the *Acd*I-*Hpa*I fragment of pRS415 (SIKORSKI and HIETER 1989; CHRISTIANSON *et al.* 1992) that contained *LEU2*. The *ADE2* marker was inserted into *III*-314 with the *Eco*RI-*Sph*I fragment of plasmid pKU7 (see below). Correct targeting of these manipulations was verified by PCR analysis of these regions at the target site and at both targeting junctions. The integration of *URA3* and *ADE2* in the targeted positions on chromosome *III* in YKU34 was also verified by meiotic mapping of the two markers with *MAT*a. The distances between *MAT*a and *URA3*, *MAT*a and *ADE2*, and *URA3* and *ADE2* were calculated as 8.0, 39, and 32 cM, respectively, which are consistent with the values of the markers mapped adjacent to them on the same chromosome in the SGD database. *E. coli* strains DH5 and DH5α were used for all plasmid manipulations.

Plasmids: Plasmid pMH116, which carried the DNA cassette for the *URA3* insertion into *III*-205, was constructed in four steps as follows. (1) The flanking regions of the target site *III*-205 were amplified separately by PCR and unique restriction sites were incorporated at both ends of the amplified fragments. From 5′ to 3′, the primers used consisted of three portions: five random sequence nucleotides followed first by six restriction site nucleotides and then by the priming sequences to amplify the relevant yeast genome region (Table 2). Primers d3W205-X and d3C205-B, used to amplify the centromere-side region of *III*-205, added an *Xba*I site at the upstream end and a *Bss*HII site at the downstream end of the fragment, respectively. Primers d3W205-B and d3C205-M amplified the telomere-side region of *III*-205 and placed a *Bss*HII site at the upstream end and an *Xma*I site at the downstream end of the fragment, respectively. The products were digested with restriction enzymes. (2) The *Xba*I-*Bss*HII and *Bss*HII-*Xma*I fragments were ligated into the *Xba*I-*Xma*I sites of plasmid pUC19 to construct plasmid pMH100. (3) The region including the *URA3* of pRS416 (SIKORSKI and HIETER 1989; CHRISTIANSON *et al.* 1992), position 187 to 1298 (GenBank accession no. U03450), was amplified by PCR with primers containing a *Bss*HII site at their 5′ ends. Primers dp416W-B and dp416C-B (Table 2) were used for this amplification. The products were digested with *Bss*HII. (4) The *Bss*HII *URA3* fragment was then inserted into the *Bss*HII site of pMH100. The resulting plasmid, which carries the *URA3* marker in the direction opposite to the *lacZ*, was designated as pMH116. It should be noted that the *Xba*I-*Xma*I fragment of pMH116 contains 41 and 39 bp of unrelated sequences upstream and downstream of the *URA3* marker between the target site, respectively. Plasmid pMJ118 was constructed by digesting pMH116 at the *Nco*I site inside the *URA3* gene, filling the site using Klenow fragment and recircularizing the DNA. A new *Eco*T22I site was created at the destroyed *Nco*I site of the *URA3* sequence in this plasmid, and the resulting *ura3* mutation was designated as *ura3-91*. Plasmid pKU7, which carried the DNA cassette for the *ADE2* insertion into *III*-314, was constructed as follows. (1) The *ADE2* coding region including possible transcription activating sequences (GEDVILAITE and SASNAUSKAS 1994) was amplified by PCR, which added an *Apa*I site at the upstream end and a *Sac*I site at the downstream end. Primers used were d15C566-A and d15W564-S (Table 2). The products were digested with *Apa*I and *Sac*I. (2) The *Apa*I-*Sac*I fragment was cloned into the *Apa*I-*Sac*I sites of pRS415 to construct the plasmid pKU4. It was confirmed that pKU4 could complement an Ade⁻ phenotype of *ade2Δ::hisG* strains. (3) The flanking regions of the target site *III*-314 were amplified separately by PCR, which incorporated unique restriction sites at each end of the amplified fragments. Primers used to amplify the centromere-side region were d3W313-E and d3C313-BK (Table 2), which added an *Eco*RI site at the upstream end and a *Kpn*I and a *Bgl*II site at the downstream end

TABLE 1

Genotypes of yeast strains

Strain	Genotype	Origin
Haploids		
FY23	*MAT***a** *leu2Δ1 ura3-52 trp1Δ63*	Fred Winston
FY838	*MAT*α *lys2Δ202 leu2Δ1 ura3-52 his3Δ200*	Fred Winston
YKU1	*MAT***a** *lys2Δ202 leu2Δ1 ura3-52 trp1Δ63*	This study
YMH1	YKU1 except *III*-205::*URA3*[a]	This study
YMJ1	FY838 except *III*-205::*URA3*	This study
YMJ2	FY838 except *III*-205::*ura3-91*	This study
YKU21	FY838 except *URA3*	This study
YMH5	YKU1 except *URA3*	This study
YMJ4	FY838 except *ura3-91*	This study
YKU23	FY838 except *ade2Δ::hisG*	This study
YKU34	YMH1 except *ade2Δ::hisG III*-314::*ADE2*[a]*LEU2*	This study
Diploids[b]		
RD101	*III*-205::*URA3/III*-205 *ura3-52/ura3-52*	YMH1 × FY838
RD102	*ura3-52/ura3-52*	YKU1 × FY838
RD103	*III*-205::*URA3/III*-205::*URA3 ura3-52/ura3-52*	YMH1 × YMJ1
RD104	*III*-205::*URA3/III*-205::*ura3-91 ura3-52/ura3-52*	YMH1 × YMJ2
RD201	*URA3/ura3-91*	YMH5 × YMJ4
RD202	*URA3/URA3*	YMH5 × YKU21
RD301	*III*-205::*URA3/III*-205 *ura3-52/ura3-52*	YKU23 × YKU34

[a] *III*-205::*URA3* signifies that the *URA3* fragment is inserted at the 205-kb position of chromosome *III*. *III*-314::*ADE2* signifies that the *ADE2* fragment is inserted at the 314-kb position of chromosome *III*. Details are described in the text.

[b] All strains are *MAT***a**/*MAT*α *lys2Δ202/lys2Δ202 trp1Δ63/TRP1 HIS3Δ200/HIS3* and, except for RD301, *leu2Δ1/leu2Δ1*. In addition, the diploid strain RD301 is *ade2Δ::hisG/ade2Δ::hisG* and has three heterozygous markers on chromosome *III*, which are *III*-205::*URA3*, *III*-314::*ADE2*, and *LEU2*. All strains are otherwise isogenic.

of the fragment, respectively. The products were digested with *Eco*RI and *Bgl*II. Primers used to amplify the telomere-side region were d3W315-BS and d3C315-S (Table 2), which added a *Bgl*II and a *Sac*I site at the upstream end and an *Sph*I site at the downstream end of the fragment. The products were digested with *Bgl*II and *Sph*I. (4) These *Eco*RI-*Bgl*II and *Bgl*II-*Sph*I fragments were cloned into the *Eco*RI-*Sph*I sites of plasmid pUC19 to construct plasmid pKU5. (5) The *Kpn*I-*Sac*I fragment of pKU4 containing *ADE2* was inserted into the *Kpn*I-*Sac*I sites of pKU5, and the resulting plasmid was designated as pKU7.

PCR procedures: All primers used in this study were supplied by Griner Japan and are listed in Table 2. PCR mixtures (25–100 μl) contained 10 mM Tris-HCl (pH 8.3), 50 mM KCl, 1.5 mM MgCl$_2$, 200 μM of each dNTP, 0.4 μM of each primer, 0.02 unit/μl of *rTaq* DNA polymerase (Takara) and 10^4–10^7 molecules of template DNA. *Ex Taq* DNA polymerase (Takara) was used instead of *rTaq* DNA polymerase to amplify the fragments for cloning. Standard PCR was performed with Gene-Amp PCR system 9600 (PE Biosystems, Foster City, CA) using a program consisting of one cycle of 1 min at 95° followed by 25 to 30 cycles of 92° for 1 min, 58° for 2 min, and 72° for 2 min, unless otherwise indicated. For amplification of DNA fragments >2 kb, the extension step at 72° was increased by 1 min for each 1-kb increase of target region. For quantitative PCR analysis of chromosome *III* (Figure 2), about 10^5 copies of yeast genomic DNA purified from PFGE plugs were used as the template in each reaction (25 μl). The primers d3W102, d3C102, d3W205, and d3C205 were added together in the same reaction. The reactions were performed with a 5-min extension step and the products were quantified after 18 or 20 cycles. For quantitative PCR analysis of chromosome *V* (Figure 4), the reaction was performed with ∼2 × 10^5 cells in a 25-μl reaction. The primer pairs used were d5W116 +

d5C117, d5W230 + d5C231, d5W543 + d5C544, and d10W587 + d10C588 and two pairs of the four were combined in the same reaction. The extension time was 3 min for all the reactions and the products were quantified at 22, 24, 26, 28, and 30 cycles. PCR analysis of the mating types was performed as described (Huxley *et al.* 1990) except that 0.02 unit/μl *rTaq* DNA polymerase and 0.4 μM of each primer were used. Primers used to analyze the loci on chromosome *III* were as follows: for *LEU2* locus, d3C92 and d3W91; for *III*-205 locus, d3W205 and d3C205; for *III*-314 locus, d3W312 and d3C314; for the Hawthorne deletion, d3W197 and d3C294.

Frequency of 5-FOA^r conversion events: For all strains examined, freshly mated diploids were used to ensure normal karyotypes were present in the starting cells. For strains except RD301, the experiments were performed as follows. Cells from a single colony were inoculated and grown overnight in SC medium depleted of uracil so as to maintain the *URA3* marker of the parent cells. A series of culture tubes with 5 ml YPD medium supplemented with 20 μg/ml uracil were each inoculated with 5 or 10^3 cells of the preculture. Uracil was added to the medium to ensure that Ura$^-$ segregants did not have a growth disadvantage due to a shortage of uracil. The frequency of 5-FOA^r cells in the inoculum was determined by plating about 10^6 cells on 5-FOA plates to make sure that the background was low. Cultures were incubated at 30° to a concentration of 5 × 10^7 cells/ml, after which the cells were harvested, washed twice, and resuspended in sterile distilled water. To disrupt the cell aggregate, either the cells were treated with 50 mM EDTA (pH 8.0) before washing or the cell suspension was briefly sonicated. The frequency of 5-FOA^r clones in each culture was determined by plating appropriate amounts of cells on two to six of both 5-FOA and YPD plates. Colonies were counted after incubation at 30° for 2 days. The 5-FOA^r colonies were classified according to size as either

TABLE 2

Nucleotide sequences of primers

Name	Priming positions (origin)[a]	Strand	Nucleotide sequences[b]
dp416W-B	152–175 (pRS416)	W	attaagcgcgcGGCATCAGAGCAGATTGTACTGAG
dp416C-B	1309–1338 (pRS416)	C	ggtatgcgcgcCTTACGCATCTGTGCGGTATTTC
dAFh505	−27 to −8 (pNKY51)	W	atggattctagaacagttggtatattgggaggggggacaattgggacgtatgattgttgagCACGAGGCCCTTTCGTCTTC
dARh2214	3845–3861 (pNKY51)	C	cttgttttctagataacgttcgtaaccgacagtttctaacttttgtgctttgacaagaacCGATGCGTCCGGCGTAG
d3W205-X	204 (chr. *III*)	W	tggcctctagATTTTAGTGCGATTTTAGAATAACTCTTGG
d3C205-B	205 (chr. *III*)	C	attacgcgcgCAATGAAATAATATGTATATGTCTACATAGAG
d3W205-B	205 (chr. *III*)	W	ttattgcgcgCTTTTTCTAATAAACGAGGAAAATGG
d3C205-M	205 (chr. *III*)	C	ggatgcccggGCTCCACTTGATGCTTCCTTATTG
d3W102	102 (chr. *III*)	W	TGGTTCGGTTGGTGCTTAGG
d3C102	102 (chr. *III*)	C	TCGTTATAATCAAAGGCGTGAGG
d3W205	205 (chr. *III*)	W	AACCCCACTTACCCCTCTGTC
d3C205-R	205 (chr. *III*)	C	TAAATTGGTGTCCCAGCAGC
d3C205	205 (chr. *III*)	C	GGCAACAGTAGGCAGTGAAAGC
d3W197	197 (chr. *III*)	W	AACTATGTCTGCAAACAGTTCTTGG
d3C294	294 (chr. *III*)	C	CATTATCAATCCTTGCATCCAGC
d3W54	54 (chr. *III*)	W	CTCACACGATCTGACTGTGACC
d3C54	54 (chr. *III*)	C	CGTAAATGGTAACATCTTCGCTG
d3W313-E	313 (chr. *III*)	W	attggtgagaattcACAGTCCAGAAGGTTACGTCATC
d3C313-BK	314 (chr. *III*)	C	cgtacgggagatctcgcggtaccTTCCGCTAGGAAGAATGTGC
d3W315-BS	314 (chr. *III*)	W	cgcgcacaagatctgcggagctcGACATATTAACGTAGGCCCGTACG
d3C315-S	315 (chr. *III*)	C	ctccaattgcatgcATCCAACTCCACCACCACTTAC
d3W91	91 (chr. *III*)	W	TCTAAGGCGCCTGATTCAAG
d3C92	92 (chr. *III*)	C	CCAGTTCTGATACCTGCATCC
d3W312	312 (chr. *III*)	W	CTCATACGATGGAGCTCGTTC
d3C314	314 (chr. *III*)	C	CGTACGGGCTACGTTAATATGTC
d5W116	116 (chr. *V*)	W	TAAGGAACGTGCTGCTACTACTCATCC
d5C117	117 (chr. *V*)	C	GTTACTTGGTTCTGGCGAGG
d5W230	230 (chr. *V*)	W	TTCACTTGCCACAACTCAGC
d5C231	231 (chr. *V*)	C	GGATAATGGCCTCATGGTACC
d5W543	543 (chr. *V*)	W	CTATTGCCAACTTCTGCGC
d5C544	544 (chr. *V*)	C	GCCTCTGATGATTGTGTAGCC
d10W587	587 (chr. *X*)	W	AACGCTTCTAACACATCACGC
d10C588	588 (chr. *X*)	C	AGCCTTCTATGCTGGAGTCG
d15W564-S	564 (chr. *XV*)	W	atttgggagctcCAAAGATATCCTGACGTAGCGC
d15C566-A	566 (chr. *XV*)	C	atttgggcccTCATGATTGATTATTACTGCTATGCTG

W, Watson strand; C, Crick strand.

[a] Numbers represent the endpoints of the priming sequences of the corresponding primer. For dp416W-B and dp416C-B, numbering is as in the GenBank database. For dAFh505 and dArh2214, numbering is as by Alani *et al.* (1987). Numbers of other primers represent the approximate positions in a kilobase scale according to the SGD database. Chromosomes and plasmids where the primer sequence is located are indicated in parentheses.

[b] Nonannealing tail sequences are in lowercase and priming sequences are in uppercase. Sequences corresponding to restriction sites added are underlined.

small (the diameter was <1 mm after 2 days) or normal-sized colonies, and the contribution of each was determined in the following experiments. 5-FOA[r] cells used for further analyses were purified on 5-FOA plates.

For strain RD301, the experiments were modified as follows. As a preculture, SC medium depleted of uracil, leucine, and adenine was used to maintain the *URA3*, *LEU2*, and *ADE2* markers of the parent cells. A total of 10[3] cells from the preculture were inoculated into a series of culture tubes with 5 ml YPAD medium supplemented with 20 μg/ml uracil. Uracil and adenine were added to the medium to ensure that Ura[−] and Ade[−] segregants did not have a growth disadvantage due to shortage of uracil and adenine. Cultures were incubated at 30° until about 3–5 × 10^{6} cells/ml were present (about 14–15 generations). About 10[6] cells were spread on three of

each of three kinds of 5-FOA plates: the usual 5-FOA plates, ones lacking leucine (5-FOA Leu[−]), and ones depleted of leucine and adenine (5-FOA Leu[−] Ade[−]). To measure the number of viable cells in the suspension, about 2 × 10^{2} cells were spread on three YPD plates. Colonies were counted after incubation at 30° for 3 days. The 5-FOA[r] cells used for further analyses were purified on the same kind of 5-FOA plates.

To determine if it was appropriate to estimate the frequency of 5-FOA[r] Leu^{−} cells as the difference between the frequencies of 5-FOA[r] cells and 5-FOA[r] Leu^{+} cells and if it was appropriate to estimate the frequency of 5-FOA[r] Leu[+] Ade^{−} cells as the difference between the frequencies of 5-FOA[r] Leu^{+} cells and 5-FOA[r] Leu[+] Ade^{+} cells, the following experiments were performed. The same number of cells was spread and grown on the three kinds of plates, 5-FOA, 5-FOA Leu[−], and 5-FOA

Leu⁻ Ade⁻. The primary 5-FOA plates were then replica plated onto 5-FOA Leu⁻ plates and the number of 5-FOAʳ Leu⁺ cells on the replicas was compared to that on the primary 5-FOA Leu⁻ plates. The ratio of the former against the latter was 1.02 ± 0.092 in experiments using four independent cultures. In a similar way, the primary 5-FOA Leu⁻ plates were replica plated onto 5-FOA Leu⁻ Ade⁻ plates and the number of 5-FOAʳ Leu⁺ Ade⁺ cells on the replicas was compared to that on the primary 5-FOA Leu⁻ Ade⁻ plates. The ratio of the former against the latter was 1.05 ± 0.22. On the basis of these results, we concluded that the frequency of 5-FOAʳ Leu⁻ cells could be estimated as the difference between the frequencies of 5-FOAʳ cells and 5-FOAʳ Leu⁺ cells. Similarly, the frequency of 5-FOAʳ Leu⁺ Ade⁻ cells was estimated as the difference between the frequencies of 5-FOAʳ Leu⁺ cells and 5-FOAʳ Leu⁺ Ade⁺ cells.

Pulsed-field gel electrophoresis: Agarose plugs of chromosomal DNA were prepared as described (SCHWARTZ and CANTOR 1984; CARLE and OLSON 1987), except that the final concentration of cells in each solid plug was between 6×10^8 and 1.2×10^9 cells/ml. Electrophoresis was performed on 1% of PFGE certified agarose (Bio-Rad) in $0.5 \times$ TBE buffer at 14° using a CHEF Mapper XA system (Bio-Rad). Chromosomes were separated at 6 V/cm of pulses angled at 120°. Switch time was linearly increased from 24.03 sec to 1 min 33.69 sec for 29 hr 57 min for standard analysis. Higher resolution around chromosome *III* and chromosome *V* was obtained by altering the switch time linearly from 24.03 to 44.69 sec for 34 hr 2 min and from 44.43 to 52.28 sec for 42 hr 46 min, respectively. After electrophoresis, the gel was stained with 0.5 μg/ml ethidium bromide for 30–60 min, destained in deionized water for 20–60 min, and photographed using a CCD video camera (Atto) with DensitoGRAPH software (Atto). Aberrant chromosome sizes were determined by comparison to normal-sized chromosomes used as standards. Copy number of chromosome *III* per cell was determined by comparison of the intensity of the corresponding band to band intensities of chromosomes *I, VI, V, VIII,* and *XI* in the same lane, using Image 1.47 software (Wayne Rasband, National Institutes of Health). The latter chromosomes serve as internal markers representing two copies of each chromosome.

Southern blotting: Gels were soaked in 0.25 N HCl for 15 min to partially depurinate the DNA and then chromosomal DNA fragments were transferred to nylon membranes (Hybond-N+, Amersham, Buckinghamshire, England) by the capillary transfer method as described (SAMBROOK *et al.* 1989) or under vacuum with a vacuum blotter Model 785 (Bio-Rad) following instructions of the manufacturer. The probes hybridizing to the left arm of chromosome *III* were generated by PCR using the primer sets d3W54 + d3C54 and d3W102 + d3C102, respectively (Table 2). The probe to detect chromosome *V* on the right arm was prepared by PCR with d5W230 and d5C231 primers (Table 2). Hybridized probes were detected with enhanced chemiluminescent direct nucleic acid labeling and detection system (Amersham) or with Gene Images labeling and detection system (Amersham) according to the protocols of the supplier.

DNA sequencing: The entire region of the PCR fragment of the *MAT-HMR* deletion was sequenced by the dye terminator method using BigDye terminator cycle sequencing kits (PE Applied Biosystems) with a capillary sequencer ABI PRISM310 (PE Applied Biosystems).

RESULTS

Frequency of functional inactivation of the *URA3* marker hemizygously inserted on chromosome *III* in diploid yeast cells: To evaluate a wide variety of events involved in the process of LOH in eukaryotic cells, especially chromosome aberrations resulting from spontaneous genetic rearrangement, we have performed direct structural analyses of genetic alterations leading to LOH in a systematic way. Our experimental design was to construct a diploid yeast strain carrying a hemizygous marker at a particular site in the genome, isolate progeny showing functional inactivation of the marker, and analyze structural features of their genome using PFGE, quantitative and qualitative PCR, and DNA sequencing. We utilized the *URA3* gene as a versatile reporter marker. When the *URA3* marker has been inactivated or lost, progeny can be positively selected because of their resistance to 5-FOA (BOEKE *et al.* 1984). Chromosome *III* was considered to be suitable as a target chromosome for our analysis because it is the yeast chromosome most extensively characterized in its structural and functional aspects (CAMPBELL and NEWLON 1991; NEWLON *et al.* 1991; RIVIER and RINE 1992; ZENVIRTH *et al.* 1992; WU and LICHTEN 1994; BAUDAT and NICOLAS 1997) and it can be separated readily from other chromosomes by PFGE.

Initially, a 1183-bp segment of DNA containing the *URA3* marker was inserted at a site 91 kb downstream from the centromere in the right arm of chromosome *III* (*III*-205::*URA3*) in a haploid strain whose authentic *URA3* gene had been inactivated. This site was chosen so as to avoid disruption of putative open reading frames. The resulting strain, YMH1 (*MAT***a** *ura3-52 III*-205::*URA3*), was then mated with another haploid strain, FY838 (*MAT*α *ura3-52*), to obtain the diploid parent strain, RD101. Then, 5-FOAʳ clones were screened from RD101 cells exponentially grown in nonselective rich medium. The average frequency of 5-FOAʳ convertants was calculated to be 2.0×10^{-4} from analyses of 23 independent cultures, each containing $5–6 \times 10^7$ cells/ml (Table 3). This frequency was 500-fold higher than the frequency of 5-FOAʳ cells determined with a haploid strain carrying the same *URA3* insert (YMH1). In similar experiments with a diploid strain homozygous for the inserted *URA3* marker (RD103), no 5-FOAʳ cells could be recovered from an average population of $5.5 \pm 2.9 \times 10^7$ cells in 9 independent cultures. Thus, the hemizygous *URA3* marker is inactivated via a mechanism specific to diploid or disomic cells.

Distribution of RD101 5-FOAʳ convertants into three classes of chromosome alterations: Chromosome patterns from a large number of 5-FOAʳ convertants from RD101 were examined by PFGE (Figure 1). To identify chromosome *III* and its derivatives, two probes specifically hybridizing with two different segments in the left arm of chromosome *III* were used in Southern blots performed with chromosomal DNA separated by PFGE. The copy number of chromosome *III* per cell was determined by comparison of the intensity of the ethidium bromide-stained band that corresponded to chromo-

TABLE 3

Frequency of 5-FOAʳ cells and clones analyzed for their chromosome structure

Strain	Genotype[a]	Mean ± SD (median) × 10^5 [class distribution (%)]			
		Total 5-FOAʳ [b]	Class A[c] chromosome loss	Class B[c] no chromosome change	Class C[c] aberrant chromosome
RD101	$\dfrac{III\text{-}205::URA3}{III\text{-}205}$	20 ± 13 (16)	13 ± 9.8 (8.5) [62]	6.7 ± 3.7 (6.8) [30]	1.1 ± 1.1 (0.71) [8.0]
RD104	$\dfrac{III\text{-}205::URA3}{III\text{-}205::ura3\text{-}91}$	16 ± 3.1 (16)	5.4 ± 3.4 (4.5) [37]	8.8 ± 1.6 (8.5) [60]	0.47 ± 0.65 (0.24) [3.2]
RD201	$\dfrac{URA3}{ura3\text{-}91}$	3.4 ± 1.4 (2.9)	0.10 ± 0.090 (0.051) [2.6]	3.7 ± 1.6 (4.1) [97]	<0.022 [<0.56]
RD103	$\dfrac{III\text{-}205::URA3}{III\text{-}205::URA3}$	<0.055	ND	ND	ND
YMH1	$III\text{-}205::URA3$	0.043 ± 0.013	ND	ND	ND

[a] Only the locus where the *URA3* marker is located in each strain is shown.

[b] The 5-FOAʳ frequency was determined with 23, 13, 10, 9, and 6 independent cultures for RD101, RD104, RD201, RD103, and YMH1, respectively.

[c] The frequencies of classes A–C are averages of those calculated for each culture from the ratios of the corresponding clones structurally analyzed as in the text. Total number of clones and cultures analyzed for the measurement was 224 clones from 6 cultures for RD101, 134 clones from 7 cultures for RD104, and 152 clones from 5 cultures for RD201. For RD101, an additional 416 clones from 12 independent cultures were analyzed for their chromosome structure and were not used to calculate the frequencies. Class distribution in each strain was listed in brackets. ND, not determined for RD103 and YMH1.

some *III* or its derivatives with those of the neighboring chromosomes in the same lane, each of which represented two copies of chromosomal DNA. Various chromosomal changes including alterations in size or loss of chromosome *III* were observed. Since the resolution limit around the position of chromosome *III* in our PFGE analyses was 5 to 10 kb, only size aberrations more than that were detectable. This also explains why the two alleles of chromosome *III* in RD101 cannot be distinguished by their migration in the gel.

On the basis of copy number and size abnormality of chromosome *III*, the 5-FOAʳ convertants could be categorized into three classes (Figure 1): class A, those retaining only one normal-sized chromosome *III*; class B, those having two normal-sized alleles of chromosome *III*; and class C, those harboring a chromosome *III* that was aberrant in size. The frequency of 5-FOAʳ clones falling into each category was determined from six independent cultures (Table 3). For each culture, 32 to 48 5-FOAʳ clones were examined for chromosome alterations. Cells monosomic for chromosome *III* (class A) were the most common and accounted for ~60% of the total clones examined. Clones harboring an aberrant chromosome *III* (class C) were found in most but not all cultures and accounted for 8% of clones. The remaining 30% of total 5-FOAʳ isolates showed no apparent alterations of either chromosome *III* or other chromosomes (class B).

Slower-growing cells present in the 5-FOAʳ convertants: During the first screening of RD101 as well as during the subsequent purification on 5-FOA plates, it

was noted that some 5-FOAʳ colonies were much smaller than others. These convertants formed colonies that had a diameter <1 mm after incubation at 30° for 2 days and accounted for 31% of all convertants. The contribution of such small colonies was <8% of the total number of colonies when the parental strain (RD101) was spread on SC plates or a *ura3/ura3* diploid strain (RD102) was grown on 5-FOA plates. To determine whether this slower growth was related to certain genetic alterations in the cells, the distribution of small colonies in each of classes A–C was examined. In all three classes, 30–40% of 5-FOAʳ clones formed small colonies, which indicated that the high incidence of slower-growing clones appeared not to be related to a certain class of genetic alteration but to be common to all classes. Among them, however, some class A and class C clones formed especially tiny colonies and their doubling time in YPD medium took up to 230 min, which was much longer than the 75 min required by the parent strain. Estimation of mutation rates from the frequency of mutants in a given population requires that the growth rate of the mutants is the same as that of parent cells (Lea and Coulson 1948; Drake 1991). If the growth rate is much reduced in a significant portion of 5-FOAʳ clones then the rate of LOH in this population may be underestimated. For this reason, we evaluated 5-FOAʳ conversion events on the basis of the frequency of the 5-FOAʳ convertants in the present study rather than the rate calculated from the frequency.

Chromosome *III* carrying the *URA3* marker is lost in class A 5-FOAʳ clones: Cells monosomic for chromo-

A Class A

Chromosome loss

P 1   P 1

B Class B

No chromosome changes

P 2   P 2

C Class C
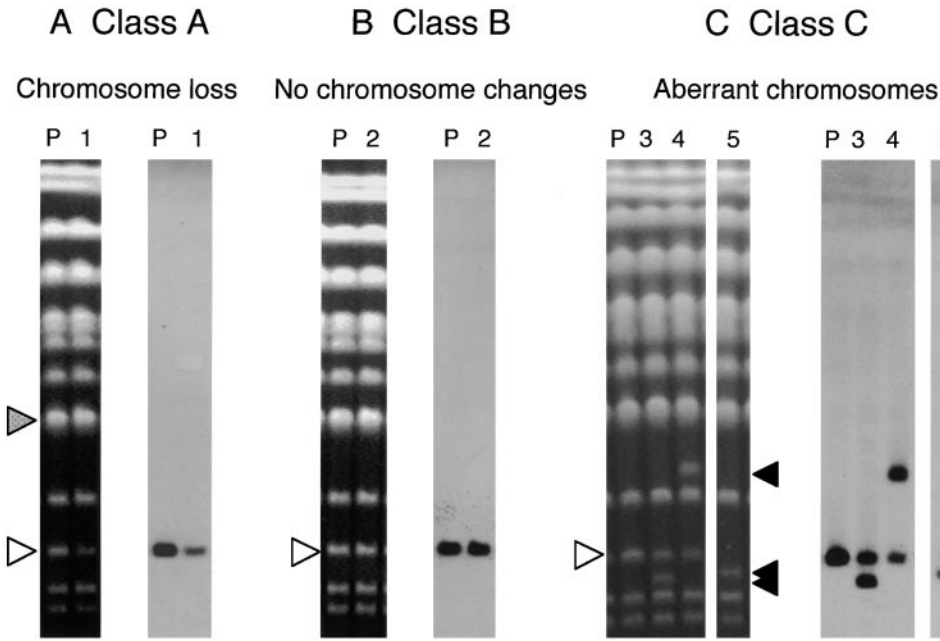
Aberrant chromosomes

P 3 4 5   P 3 4 5

FIGURE 1.—Classification of 5-FOA[r] cells based on the copy number and the size abnormality of chromosome *III* as detected by PFGE and Southern blotting. (A–C) The pattern of chromosomes in representative clones of each class (for classification, see text) relative to that of parental strain RD101 (marked with P). The left half of each shows an ethidium bromide-stained gel of PFGE; the right half shows Southern blotting analysis of the same gel. Bands corresponding to the authentic chromosome *III* are marked by open arrowheads; aberrant chromosomes derived from chromosome *III* are marked by solid arrowheads. Bands corresponding to chromosomes *V* and *VIII* are marked by a shaded arrowhead.

some *III* (class A) were further examined to confirm that 5-FOA resistance in these cells was due to loss of the chromosome. We determined which of the parental chromosome *III* pair, the chromosome inserted with the *URA3* marker or the unaltered chromosome, was lost in the class A clones by determining the presence of *MAT*a with PCR (HUXLEY *et al.* 1990). *MAT*a/*MAT*α is a heterozygous marker in the parent strain RD101 and is closely linked to the *URA3* marker on chromosome *III*. *MAT*a is located ∼5 kb from the *URA3* marker on its centromere side in the same chromosome. In all 376 class A clones, the *MAT*α but not the *MAT*a locus could be amplified by PCR. Thus, the functional inactivation of the *URA3* marker in the monosomic clones is due to loss of the chromosome *III* carrying the inserted *URA3* and *MAT*a markers.

Class B 5-FOA[r] clones were homozygous wild type for the *III*-205 locus: According to previous LOH studies with diploid or partial diploid yeast cells (CAMPBELL *et al.* 1975; MALONE *et al.* 1980; ESPOSITO *et al.* 1982, 1994; HARTWELL and SMITH 1985; SUROSKY and TYE 1985; MEEKS-WAGNER and HARTWELL 1986; KUPIEC and PETES 1988; BRUSCHI *et al.* 1995), class B clones, the second most frequent class of RD101 5-FOA[r] convertants, were expected to be generated by recombination between allelic chromosomes followed by segregation of the recombinant chromosomes during mitosis. However, because the PFGE technique used here could not reveal chromosomal size changes <5 kb, we were unable to rule out the involvement, in class B clones, of genetic alterations that yielded size alterations <5 kb such as deletions, insertions, duplications, and point mutations in the *URA3* marker. To identify such genetic alterations, we performed PCR-based structural analyses of the local DNA configuration around the *URA3* marker.

Attempts were made to amplify the marker sequence in the genomes of class B clones with primers that specifically annealed with sequences at both ends of the inserted *URA3* marker. Although the expected size fragment could be generated when genomic DNA from the parent strain was used, the *URA3* marker could not be amplified from DNA of any of 27 class B clones examined. Thus, the entire inserted segment that contained the *URA3* marker was most likely lost in the class B clones.

The sequences surrounding the *URA3* marker were then examined using primers positioned on both sides of the *URA3* insertion site, *III*-205 (Figure 2, primer set B). To permit quantification of this amplification, primers that amplified a sequence on the left arm of
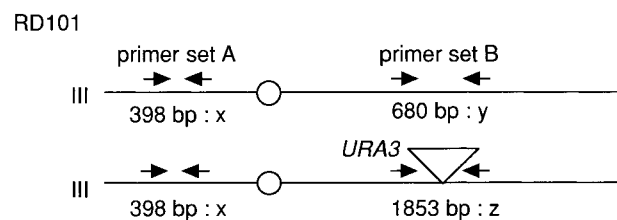
RD101

FIGURE 2.—Analysis of the *III*-205 locus by quantitative PCR. The chromosome *III* pair of parent strain RD101 is illustrated with relative positions of primers used. Two horizontal lines depict the chromosome pair, circles indicate their centromeres, and an open triangle marks the *URA3* insert at the *III*-205 locus. Head-to-head pairs of arrows indicate PCR primer sets. PCR product lengths resulting from each primer set are indicated below the corresponding positions. Three PCR products were amplified from the parental strain and are designated as fragments x, y, and z as indicated. Primer sets A and B are, respectively, d3W102 and d3C102, and d3W205 and d3C205 pairs shown in Table 2, all of which are added together in the same reaction.

chromosome *III* (primer set A) were added to the same reaction mixture to generate an internal control (fragment x). Reaction conditions were adjusted so that the reaction was terminated within the phase of exponential amplification (18–20 cycles with 3 ng of genomic DNA). When genomic DNA from the parent strain RD101 was used as the template, a 1853-bp DNA fragment (fragment z) that included the *URA3* marker and a 680-bp DNA fragment (fragment y) that corresponded to the allelic locus without the marker were amplified. The molecular ratio of y/x was 0.43. When a control diploid strain that was homozygous wild type for the *III*-205 locus (RD102) was used, the y/x ratio was 0.80, about twice that of the parent strain. For all 213 class B clones isolated, fragment y but not fragment z could be amplified and the ratio of y/x was ∼0.80. These results clearly indicated that the inserted DNA segment that contained the *URA3* marker was absent from the genome of class B convertants and that locus *III*-205 in these convertants was homozygous wild type. Since no clones in class B contained point mutations and structural alterations such as deletions and insertions <5 kb, their frequency in overall 5-FOA^r conversion was estimated to be lower than 3.1×10^{-7}. Thus, we concluded that there was little, if any, involvement of such alterations in the functional loss of the *URA3* marker in RD101.

The loss of the *URA3* marker in class B clones might be due to its replacement with the allelic locus through gene conversion around the site or crossing over in the *CEN III-URA3* interval. It is also possible that the chromosome *III* that carried the *URA3* marker was lost and the remaining chromosome *III* reduplicated. These possibilities were tested by examination of the *MAT* locus of the 213 class B clones by PCR (Huxley *et al.* 1990). Of these clones, 39 retained both the *MAT***a** and *MAT*α loci, while the remaining 174 lost the *MAT***a** locus that was closely linked with the inserted *URA3* marker. Thus, in the former clones, the *URA3* marker was most likely lost through allelic recombination, either by gene conversion localized around *III*-205 locus or by crossing over in the interval between *III*-205 and *MAT* loci. In the latter clones, however, while recombination may also have been responsible for the loss of the *URA3* marker through allelic crossing over in the *CEN III-MAT* interval, the possibility that chromosome loss with reduplication occurred cannot be excluded.

There are three distinct subtypes of class C 5-FOA^r clones carrying an aberrant chromosome: As summarized in Table 4, 51 clones that carried an aberrant chromosome *III* (class C) were identified in 640 5-FOA^r convertants from RD101. The aberrant chromosomes varied widely in size from 110 kb smaller to 620 kb larger than the normal chromosome *III*. The aberrant chromosome in ∼80% of the clones was smaller than the normal chromosome. In the remaining clones it was much larger, the largest being almost three times

TABLE 4

Aberrant chromosomes of class C clones from RD101

Size change^a (kb)	No. of clones identified	No. of cultures identified	*III*-205 locus on the aberrant chromosome^b
−110	1	1	−
−105	2	1	−
−100	1	1	−
−80	15	9	−(ND for 2 clones)
−60	7	2	−
−55	3	2	−
−50	5	4	−(ND for 1 clone)
−40	2	2	+
−30	4^c	4	+
−25	1	1	−
−10	1^d	1	+
+110	1	1	−
+145	1	1	−
+210	1	1	−
+250	1	1	−
+340	2	2	ND
+380	2	2	−
+620	1	1	ND
Total	51	9	

^{a} The length of the aberrant chromosome was determined by PFGE and the size difference between it and the 330-kb wild-type chromosome *III* is indicated.

^{b} Presence (+) or absence (−) of the *III*-205 locus on the aberrant chromosome was determined by quantifying the locus with PCR as shown in Figure 2. ND, not determined because of loss of the clone during storage.

^{c} In two cases out of four, the other normal-sized chromosome *III* could not be identified (the third subtype in the text).

^{d} The normal-sized chromsome *III* was not identified (the third subtype in the text).

as big as the normal chromosome. We have noticed that multiple clones carried an aberrant chromosome *III* that was indistinguishable by size. Among these, clones carrying an 80-kb shorter chromosome *III* occurred most frequently and accounted for 29% of all class C clones examined. Although these chromosomes might have different endpoints, it is probable that there are certain "hot spots" involved in generating class C clones in chromosome *III*.

To obtain an insight into the mechanisms generating the class C clones, we examined the DNA arrangement around locus *III*-205, where the *URA3* marker was inserted, using the quantitative PCR analysis as described for class B clones (Figure 2). All class C clones, apart from six that could not be recovered after storage, were tested and could subsequently be further classified into three subtypes (Table 4).

The first subtype was characterized by gross deletion of the inserted *URA3* marker and its flanking DNA. The majority of clones, 38 of 45, fell into this category. In these clones, fragment y but not fragment z could be

amplified, and the molecular ratio of y/x was ∼0.43, similar to that of the parental strain. Thus, in these clones, locus *III*-205 became hemizygous upon losing the inserted marker. Despite deletions encompassing the *URA3* marker, all six class C clones carrying larger aberrant chromosomes fell into this subtype. Such aberrant chromosomes were probably generated by the rejoining of a large segment of DNA at a site between the *CEN III-URA3* interval.

The second subtype was characterized by replacement of the DNA segment that contained the inserted *URA3* marker with wild-type locus *III*-205. Four of the remaining seven clones fell into this category. In these clones, fragment y but not fragment z could be amplified, and the molecular ratio of y/x was ∼0.80, similar to that of a homozygous control strain. These clones are thus probably homozygous wild type for locus *III*-205. This subtype might be related to class B clones and was probably generated by unequal crossing over between the *CEN III-URA3* interval. Consistent with this notion was the finding that the decrease in size of the aberrant chromosomes of these clones was relatively small (40 or 30 kb; Table 4).

The remaining three clones fell into the third subtype, characterized by the presence of an aberrant chromosome *III* and the loss of the other chromosome *III* (an example is shown in lane 5 of Figure 1C). In these clones, the DNA segment containing the *URA3* marker has been replaced with wild-type locus *III*-205, similar to what is seen in clones from the second subtype. With these clones that carried a single chromosome *III*, 30 or 10 kb smaller than the normal chromosome, fragment y but not fragment z could be amplified by PCR. The y/x ratio was ∼0.80. These clones are thus hemizygous for locus *III*-205 and are related to both class A clones and the second subtype of class C clones. It is likely that the aberrant chromosomes were generated, like the second subtype of class C clones, by unequal crossing over between the *CEN III-URA3* interval.

Loss of heterozygosity of the *URA3* marker in *III*-205::*URA3*/*III*-205::*ura3-91* diploid cells: In the RD101 diploid strain, the insertion of the *URA3* marker results in substantial size heterogeneity between the two *III*-205 loci. This situation is somehow different from usual LOH in carcinogenesis, and it is possible that the large difference in loci in our experimental model might affect the pattern of LOH in diploid yeast cells. This was tested by experiments using RD104, a diploid strain with almost identical chromosome *III*s (Figure 3A). In this strain, one chromosome *III* is derived from YMH1 and carries *URA3*, while the other chromosome comes from YMJ2 and contains *ura3-91*, a sequence obtained by introducing a single-base frameshift mutation at the *NcoI* site in the wild-type *URA3* sequence. The mutation completely abolishes *URA3* gene function and simultaneously creates an *Eco*T22I site.

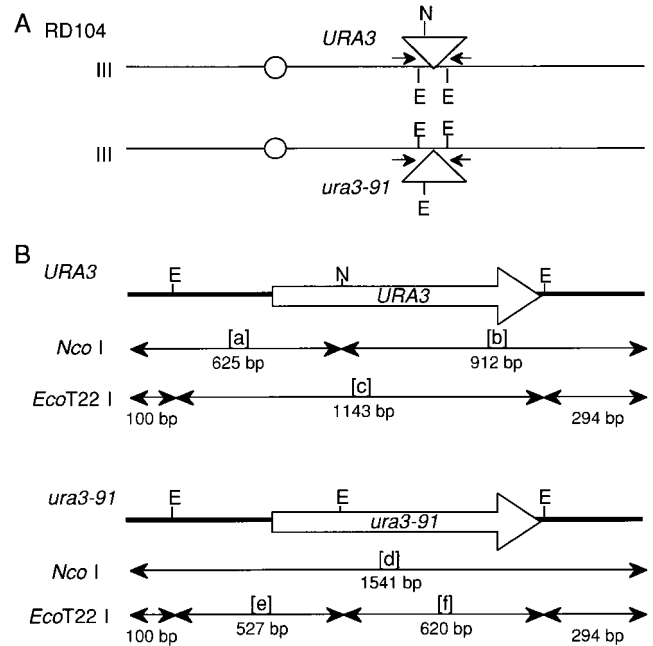With this strain, the average frequency of 5-FOA^r con-

FIGURE 3.—RFLP analysis of the *III*-205 locus in class B clones from the least heterozygous diploid strain, RD104. (A) Schematic depiction of the chromosome *III* pair of parent strain RD104 showing the relative positions of the primers used. Two horizontal lines depict the chromosome pair, circles indicate their centromeres, and open triangles mark the *URA3*/*ura3-91* inserts at the *III*-205 locus. Head-to-head pairs of arrows indicate the primer set d3W205 and d3C205-R (Table 2), which amplifies the *III*-205 locus. E and N represent *Eco*T22I and *Nco*I sites in the amplified regions, respectively. (B) An expanded view of the region amplified by PCR, shown in A, for each allele. The *URA3*/*ura3-91* inserts are shown by open bars with arrowheads indicating the direction of transcription. Thick lines represent the surrounding sequence at *III*-205. E and N represent *Eco*T22I and *Nco*I sites, respectively. The restriction fragments of the PCR products digested with either *Nco*I or *Eco*T22I are shown by thin lines with two arrowheads for each allele as indicated. Restriction fragment lengths are indicated below the corresponding lines. The six fragments (a–f) indicate the two alleles.

vertants, obtained from analyses of 13 independent cultures each containing 5.9 × 10^7 cells/ml, was 1.6 × 10^−4, similar to that obtained with RD101 (Table 3). The RD104 5-FOA^r convertants could also be classified into classes A–C according to their chromosome patterns, but the frequencies of clones falling into each class differed from those seen with RD101. Clones with a loss of a chromosome *III* (class A) occurred less frequently, while class B clones, which had two normal-sized chromosome *III*s, occurred slightly more frequently. As a result, class B became the most abundant class of 5-FOA^r convertants. Eight clones from 134 5-FOA^r convertants from RD104 contained an aberrant chromosome *III* (class C) and, thus, the frequency of class C was comparable with that for RD101. The number of class C clones obtained was, however, too small to determine the distribution of subtypes in these clones.
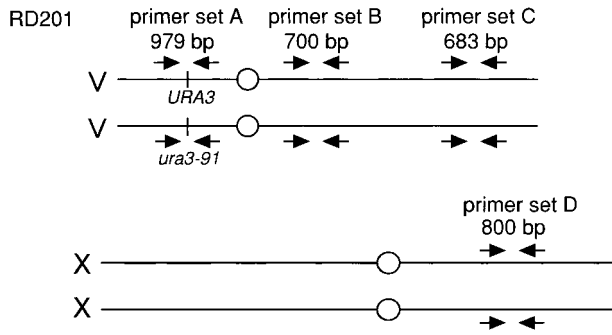
FIGURE 4.—Determination of copy number of chromosome *V* with quantitative PCR. Chromosomes *V* and *X* in parent strain RD201 are schematically depicted with relative positions of the primers used. Two horizontal lines depict a chromosome pair and circles indicate their centromeres. Head-to-head pairs of arrows indicate primer sets A–D. PCR product lengths with each primer set are indicated above the corresponding positions. Primer sets A–D consist of the d5W116 and d5C117, d5W230 and d5C231, d5W543 and d5C544, and d10W587 and d10C588 primers (Table 2), respectively.

Thus, the chromosomal changes leading to loss of *URA3* function in RD104 occur in essentially the same manner as for RD101. However, the decrease in prevalence of class A clones in RD104 suggests that the large heterogeneity between the chromosome *III* pair in RD101 might enhance, by two- to threefold, the occurrence of the mechanism leading to loss of the chromosome.

ura3-91 could be easily identified through its unique restriction enzyme digestion pattern, allowing further examination of the nature of the LOH in the RD104 class B clones, which might have two *ura3-91* chromosome *III*s. The replacement of *URA3* with *ura3-91* means that the PCR product of the *URA3* sequence becomes totally resistant to *Nco*I digestion and would be completely digested into four fragments by *Eco*T22I (Figure 3B). Analysis of the PCR products with the restriction enzymes showed that all 69 class B clones isolated from seven independent cultures had lost the wild-type *URA3* sequence and carried only the *Nco*I-resistant *ura3-91* sequence.

Loss of heterozygosity of the autologous *URA3* marker located on chromosome *V*: To gain a more generalized view of chromosome instability as well as to measure its variability between individual chromosomes, LOH of the same marker on another chromosome was examined. Chromosome *V* was used for this analysis because it carries the autologous *URA3* gene, which is ~35 kb upstream from its centromere on the left arm.

RD201 is a diploid strain heterozygous for the *URA3* locus on chromosome *V* and was constructed by mating a *URA3* wild-type haploid strain, YMH5, with another haploid strain, YMJ4, which carries the *ura3-91* mutation at the authentic locus (Figure 4). The frequency of total 5-FOA^r convertants in logarithmically growing cultures of RD201 (an average titer of 4.0×10^7 cells/ml) was 0.34×10^{-4}, five times lower than that observed for

RD104 (Table 3). The chromosome patterns of the convertants were examined in a way similar to those of the RD101 and RD104 convertants. Chromosome *V* could not be well separated from chromosome *VIII* in PFGE (Figure 1), but this was resolved by using Southern hybridization of DNA separated in PFGE with a probe specific for a DNA sequence on the right arm of chromosome *V*. This analysis, with a resolution limit of ~10 kb around the position of chromosome *V*, showed that this chromosome in all of 152 5-FOA^r clones isolated from five independent cultures was not altered in size. Thus, the occurrence of class C clones in RD201 was at an undetectable level, estimated to be below 2.2×10^{-7}, and all clones fell into either class A or B.

Since the hybridization analyses did not allow precise measurement of chromosome *V* copy number, quantitative PCR was performed to distinguish between class A and B clones (Figure 4). The relative copy number was estimated for four loci in the yeast genome: the *URA3* locus, two loci on the right arm of chromosome *V*, and a locus on chromosome *X* that served as a standard diploid locus. Of 152 5-FOA^r clones examined, 119 clones were classified as class B that carried a pair of chromosome *V*s and the remaining 33 were classified as class A in which either one of the chromosome *V* pair was lost.

Using the PCR-based restriction fragment length polymorphism analysis, as performed with class B clones from RD104 (Figure 3), we determined which allele was retained at the *URA3* locus in both class A and class B convertants from RD201. PCR products of the *URA3* locus (Figure 4) were digested with either *Nco*I or *Eco*T22I. All of 33 class A and 119 class B clones were examined, and each carried only the *Nco*I-resistant *ura3-91* allele. We concluded that the class A clones had lost the chromosome *V* carrying *URA3*, while the class B clones became homozygous for *ura3-91*.

Table 3 summarizes the distribution of the 5-FOA^r convertants from RD201 into classes A–C. When compared to RD104 and RD201, it was clear that the frequencies of two of the three major chromosomal alterations that led to LOH varied significantly when the genetic marker concerned was located in different chromosomes. That is, loss of chromosome *V* occurred 50-fold less frequently than loss of chromosome *III*, and size aberrations of chromosome *V* that resulted in LOH were at least 21-fold less frequent than that of chromosome *III*. On the other hand, frequencies of class B clones were at a similar level and the ratio of those in RD104 and RD201 was 2.4. This agrees well with the ratio of *URA3-CEN* interval size on chromosomes *III* and *V*, which is 2.6. This result suggested that class B clones resulted mainly from crossing over and that their prevalence was correlated with the distance between the given locus and its centromere.

Experimental approaches to understanding the origins of aberrant chromosomes generated in diploid

yeast cells: In the experiments described above, we identified clones with aberrant chromosomes (class C) by directly analyzing chromosome patterns of many 5-FOA^r convertants with PFGE and Southern blotting. The method proved to be effective for this purpose and an aberrant-sized chromosome *III* was identified in ∼6–8% of the 5-FOA^r convertants from RD101 or RD104 (Figure 1; Table 3). These clones could be subdivided into at least two distinct types based on the status of *III*-205 locus that was analyzed by PCR (Table 4). However, it seemed difficult to apply these procedures for statistical measurements of such fluctuating events unless we analyzed a large number of convertants from several independent populations. Moreover, structural analyses of the aberrant chromosomes identified in this way were available only with physical methods such as competitive PCR. To gain a more definite insight into the mechanisms generating aberrant chromosomes and to determine more precisely the frequencies of these distinct events leading to the chromosome aberrations, we improved our previous experimental system by introducing two other heterozygous markers besides *URA3* into chromosome *III*.

A new parental strain, RD301, was constructed by mating a haploid strain YKU34 (*MATa ura3-52 ade2Δ::hisG LEU2 III*-205::*URA3 III*-314::*ADE2*) with another haploid strain, YKU23 (*MATα ura3-52 ade2Δ::hisG leu2Δ1*) (Figure 5). The *LEU2*, *ADE2*, and *URA3* markers are located on the same chromosome in this diploid strain. Intrinsic *LEU2* serves as a marker indicating the status of the left arm. Our definition of aberrant chromosome *III* is a chromosome showing a size different from the normal chromosome *III* but maintaining the left arm and the centromere of chromosome *III*. Thus, the aberrant chromosome *III* accompanied by the loss of the *URA3* marker should maintain the *LEU2* marker. Since 5-FOA^r convertants with simple loss of the chromosome *III* carrying the *URA3* marker are expected to lose all three markers simultaneously (Figure 5A), this class of clones (class A), which accounts for more than half of the total LOH$^+$ clones, can be selectively eliminated using a medium depleted of leucine. *ADE2*, inserted on the telomere side of the last ORF in the right arm of chromosome *III*, serves as a marker indicating the status of the region distal from the *URA3* marker. By following the fate of these two markers in the 5-FOA^r convertants, it is possible to trace the way in which the original chromosome *III* is rearranged to produce aberrant chromosomes. If aberrant chromosomes result from intrachromosomal deletion of the DNA segment containing the *URA3* marker, both *LEU2* and *ADE2* markers can be maintained in the resulting chromosome (Figure 5C). Thus, this type of aberrant chromosome would be found frequently in 5-FOA^r Leu$^+$ Ade$^+$ clones. On the other hand, when the *URA3* marker is lost as a consequence of interchromosomal interactions, either by unequal crossing over between homologous chromosome
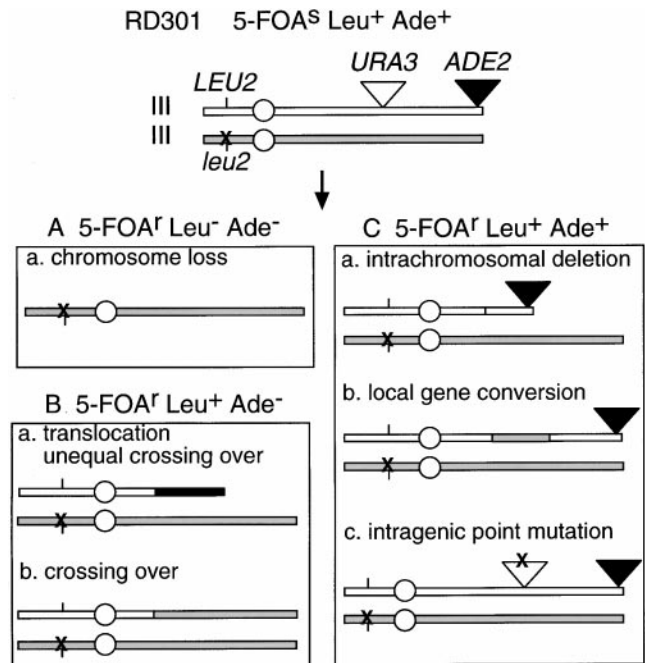

FIGURE 5.—Classification of genetic alterations leading to functional inactivation of the *URA3* marker in strain RD301. Chromosomes *III* in parent strain RD301 (top) and their possible alteration in 5-FOA^r convertants (bottom) are illustrated with relative positions of the three markers used for the analysis. The 5-FOA^r convertants are classified with their indicated phenotypes (A–C) and with alteration patterns of chromosome *III* (a–c), which are distinguished as shown in Figure 1. The segments of chromosome *III* originally harboring the markers are shown by open bars and those of the homologous chromosome *III* are shown by shaded bars with their centromeres as circles. A solid bar in B-a indicates a chromosome segment translocated to the marked chromosome *III* from another chromosome. The *URA3* insert at *III*-205 is indicated by an open triangle, the *ADE2* insert at *III*-314 is shown by solid triangles, and the positions of intrinsic *LEU2* loci are indicated by vertical lines, which are marked with a cross for the *leu2* allele. A point mutation inactivating the *URA3* insert is shown by a cross on the open triangle.

*III*s or by translocation with another chromosome, the *ADE2* marker would also be lost while the *LEU2* marker would remain in the resulting aberrant chromosome (Figure 5B). In this case, such aberrant chromosomes would be detected often in 5-FOA^r Leu$^+$ Ade$^-$ convertants.

In a similar way, two distinct types of allelic recombination, both of which result in two normal-sized chromosome *III*s that are homozygous for *III*-205 in 5-FOA^r convertants (class B), can also be distinguished using the new parental strain. If the chromosome has lost the *URA3* marker by local gene conversion not associated with crossing over, such convertants would maintain the *LEU2* and *ADE2* markers and show a phenotype of 5-FOA^r Leu$^+$ Ade$^+$ (Figure 5C). Meanwhile, crossing over between homologous chromosome *III*s in the interval from *III*-205 to the centromere will give rise to a hybrid chromosome *III* in which the telomere-side re-

TABLE 5

Frequency of 5-FOAʳ convertants from the parent strain RD301 and the association of these convertants with Leu and Ade markers

| Phenotypes | Frequency ($\times 10^5$) | | Ratio (%) |
	Mean $\pm$ SD	Median	
5-FOAʳ	17 $\pm$ 14	12	100
5-FOAʳ Leu$^+$	7.2 $\pm$ 6.3	5.2	43
5-FOAʳ Leu$^+$ Ade$^+$	0.56 $\pm$ 0.65	0.35	2.9
5-FOAʳ Leu$^-$	9.8	6.8	57
5-FOAʳ Leu$^+$ Ade$^-$	6.6	4.9	41

The frequencies of the cells converted to 5-FOAʳ, 5-FOAʳ Leu$^+$, and 5-FOAʳ Leu$^+$ Ade$^+$ were measured with 15 independent cultures. Cells were inoculated at ~10^3 cells into 5 ml medium and the cultures were incubated for an average of 14.2 $\pm$ 0.3 generation times. The frequency of 5-FOAʳ Leu$^-$ clones was calculated by subtracting the frequency of 5-FOAʳ Leu$^+$ clones from that of 5-FOAʳ cells. Similarly, the frequency of 5-FOAʳ Leu$^+$ Ade$^-$ clones was calculated by subtracting the frequency of 5-FOAʳ Leu$^+$ Ade$^+$ clones from that of 5-FOAʳ Leu$^+$ (see materials and methods).

gion of the right arm containing both *URA3* and *ADE2* markers is replaced with the corresponding wild-type sequence of another chromosome *III*. LOH$^+$ clones with this type of allelic recombination would show a phenotype of 5-FOAʳ Leu$^+$ Ade$^-$ (Figure 5B). Gene conversion that replaced the segment that contained the *URA3* with the wild-type sequence and was accompanied by crossing over in the interval from *URA3* to *ADE2* would also be included in this kind of convertant.

We expected allelic recombination to occur more frequently than chromosome aberrations in our system. Hence, we first determined the phenotypes of the 5-FOAʳ convertants as either Leu$^+$ Ade$^+$ or Leu$^+$ Ade$^-$ and then determined the size of their chromosomes using PFGE to distinguish clones with the chromosome aberration from those with the allelic recombination.

Frequencies of 5-FOAʳ Leu$^+$ Ade$^+$ and 5-FOAʳ Leu$^+$ Ade$^-$ convertants in the diploid cells carrying three heterozygous markers on chromosome *III*: With the new parental diploid strain RD301, we first determined the frequency of 5-FOAʳ convertants in the cells growing exponentially in nonselective rich medium. From experiments with 15 independent cultures, final titers of which were set around 4×10^6 cells/ml, the frequency of 5-FOAʳ convertants was calculated to be 1.7×10^{-4} in arithmetical mean and 1.2×10^{-4} in median (Table 5). As expected, these numbers were comparable to those obtained with the strain RD101 that carried the same *III*-205::*URA3* insert (Table 3). Cells from the same cultures were spread on 5-FOA plates lacking leucine and ones depleted with leucine and adenine to measure the frequencies of 5-FOAʳ Leu$^+$ and 5-FOAʳ Leu$^+$ Ade$^+$ clones, respectively (Table 5). In these experiments, we could examine the phenotypes of a large number of

clones in multiple cultures, which enabled the calculation of the median frequencies. Because the frequency estimated from the arithmetical mean is overly influenced by the jackpot effect, we used the median to express the frequency of clones concerned for analyses with RD301.

5-FOAʳ convertants accompanied by the Leu$^-$ or Ade$^-$ phenotype cannot be directly screened with the selective plates. Instead, we calculated the frequency of 5-FOAʳ Leu$^-$ clones by subtracting the frequency of 5-FOAʳ Leu$^+$ clones from that of 5-FOAʳ cells (Table 5). The calculated frequency of 5-FOAʳ Leu$^-$, 6.8×10^{-5}, is comparable to the frequency of clones monosomic for chromosome *III* (class A) determined with the strain RD101 (Table 3). Similarly, the frequency of 5-FOAʳ Leu$^+$ Ade$^-$ clones was calculated by subtracting the frequency of 5-FOAʳ Leu$^+$ Ade$^+$ clones from that of 5-FOAʳ Leu$^+$ cells. The calculated frequency of 5-FOAʳ Leu$^+$ Ade$^-$ clones is 4.9×10^{-5}. Since the 5-FOAʳ Leu$^+$ Ade$^-$ clones were expected to result from interchromosomal rearrangements, either by crossing over between homologous chromosome *III*s or by translocation with another chromosome (Figure 5B), such interchromosomal rearrangements appeared to be involved in about half of the LOH events that led to the functional inactivation of the *URA3* marker.

Aberrant chromosomes resulting from intrachromosomal recombination: As described above, 5-FOAʳ Leu$^+$ Ade$^+$ convertants result from genetic alterations inactivating the *URA3* marker without affecting the other two markers. Expected events leading to this genetic alteration are intrachromosomal rearrangements of the DNA segment including the *URA3* marker, gene conversion localized around the marker, and point mutations in the marker (Figure 5C). In fact, PFGE analyses of these convertants, performed as for those of RD101 (Figure 1), revealed two types of clones showing different chromosome patterns: (1) clones having two normal-sized chromosome *III*s (class B) and (2) those carrying an aberrant-sized chromosome *III* along with a normal-sized one (class C). Table 6A shows the distribution of 98 5-FOAʳ Leu$^+$ Ade$^+$ convertants into these two classes. All class B clones were further examined for their status of locus *III*-205 using quantitative PCR similar to the analysis performed for RD101 (Figure 2). Nine of the 11 clones appeared to be homozygous for the wild-type allele (non-*URA3* insertion) of locus *III*-205. Thus, we concluded that 5-FOAʳ Leu$^+$ Ade$^+$ class B clones result mainly from gene conversion around locus *III*-205. The remaining two clones that were isolated from the same culture were found to carry an identical point mutation (G:C to T:A base substitution) within the *URA3* marker and thus probably are siblings. This result indicates that the frequency of point mutations in the *URA3* marker would be at least five times lower than the frequency of gene conversion. In 87 class C clones (Table 6A), on the other hand, the aberrant

TABLE 6

Classification of 5-FOA^r Leu$^+$ Ade$^+$ clones (A) and 5-FOA^r Leu$^+$ Ade$^-$ clones (B) based
on the copy number and the size abnormality of chromosome *III*

Copy number					
Authentic chromosome *III*	Aberrant chromosome *III*	No. of clones identified	No. of cultures identified	Ratio (%)	Frequency (×10^{-5})
		A. 5-FOA^r Leu$^+$ Ade$^+$ clones			
2	0	Class B 11	6	11	0.039
1	1	Class C 87	8	89	0.31
		Total 98	8	100	0.35
		B. 5-FOA^r Leu$^+$ Ade$^-$ clones			
2	0	Class B 115	7	82	4.0
1	1	Class C 18	5	13	0.63
1	0	Class A 7	3	5.0	0.25
		Total 140	7	100	4.9

For 5-FOA^r Leu$^+$ Ade$^+$ clones (A), 98 clones were randomly chosen from eight independent cultures and analyzed with PFGE and Southern blotting as described in MATERIALS AND METHODS. For 5-FOA^r Leu$^+$ Ade$^-$ clones (B), 140 isolates from seven independent cultures were analyzed in a similar way. The frequency of each class was estimated by multiplying the frequency of total 5-FOA^r Leu$^+$ Ade$^+$ cells (0.35 × 10^{-5}) or of total 5-FOA^r Leu$^+$ Ade$^-$ cells (4.9 × 10^{-5}) by the corresponding ratio, respectively.

chromosomes probably resulted from intrachromosomal deletions of DNA segments that included the *URA3* marker.

Interestingly, all of the aberrant chromosomes identified in the class C clones migrated to a similar position in PFGE that corresponded to a size ~80 kb smaller than the normal chromosome *III*. On the basis of this result, we expected that the aberrant chromosome might arise due to the Hawthorne deletion, a recessive lethal deletion between *MAT* and *HMR* loci located ~90 kb apart in the right arm of chromosome *III* (HAWTHORNE 1963). Since the DNA segment that would be eliminated by Hawthorne deletion includes locus *III*-205 but not locus *III*-314, such a deletion occurring in the chromosome *III* of RD301 would produce a chromosome missing the *URA3* marker only. To examine this possibility, PCR encompassing a segment between *MAT* and *HMR* was carried out with DNA from 5-FOA^r Leu$^+$ Ade$^+$ class C clones. PCR with the 87 clones successfully amplified the 3.0-kb fragment indicative of Hawthorne deletion in all cases. Furthermore, DNA sequence analysis of the PCR products revealed that the 1.6 kb of homologous sequence of *MAT*a and *HMR* was faithfully fused within the amplified DNA, as in the case of Hawthorne deletion. From these results, we concluded that all of the aberrant chromosomes identified in the 5-FOA^r Leu$^+$ Ade$^+$ convertants resulted from intrachromosomal recombination between *MAT*a and *HMR* with a frequency of 3.1 × 10^{-6} (Table 6A). This is the first report on the frequency of Hawthorne deletion in a heterothallic diploid strain, while the frequency in homothallic strains that maintain active HO endonuclease has been previously reported as ~1% (HABER *et al.* 1980).

The aberrant chromosome caused by Hawthorne deletion was similar in size to the most frequent type of aberrant chromosome isolated from the strain RD101 (Table 4). Although it is not clear whether these chromosomes resulted from intrachromosomal rearrangement, the same PCR used to detect Hawthorne deletion successfully amplified the 3.0-kb fragment with 11 of the 13 clones. The frequency of such clones in RD101 was about 3 × 10^{-6}, which is in good agreement with the frequency of Hawthorne deletion observed with RD301.

Aberrant chromosomes resulting from interchromosomal rearrangement: 5-FOA^r Leu$^+$ Ade$^-$ convertants formed red colonies on 5-FOA Leu$^-$ plates and could be easily distinguished from 5-FOA^r Leu$^+$ Ade$^+$ clones, which formed white colonies on the same plates (ROMAN 1956). We isolated 140 5-FOA^r Leu$^+$ Ade$^-$ clones from seven independent cultures of RD301 by picking 20 clones from each culture. Chromosomes from all the clones were examined by PFGE analysis. We identified three types of clones with different chromosome patterns (Table 6B): (1) clones having two normal-sized chromosome *III*s (class B), (2) those carrying an aberrant-sized chromosome *III* along with a normal one (class C), and, unexpectedly, (3) those monosomic for chromosome *III* (class A), which is described in detail below. The class B clones were considered to arise from crossing over between homologous chromatids of chromosome *III* in the interval from locus *III*-205 to the centromere (Figure 5B). Their estimated frequency, 4.0 × 10^{-5}, was comparable to the frequency of class B convertants from the strain RD101 (Table 3).

Aberrant chromosomes identified in 5-FOA^r Leu$^+$ Ade$^-$ clones were expected to result from either unequal crossing over between homologous chromosome

*III*s or translocation with another chromosome (Figure 5B). In fact, sizes of aberrant chromosomes identified in 18 class C clones varied widely. The distribution was similar to that observed with RD101 (Table 4), except that an 80 kb shorter chromosome *III*, the one most frequently recovered from RD101, was not obtained in 5-FOA^r Leu$^+$ Ade$^-$ clones. These class C clones were further examined for their status of locus *III*-205 by quantitative PCR as used for RD101 (Figure 2). Of 18 clones, 1 clone was homozygous for the wild-type allele (non-*URA3* insertion) of locus *III*-205, which suggested the involvement of unequal crossing over between the homologous chromosome *III*s. Consistent with this idea was the finding that the aberrant chromosome had a small change in size and was 10 kb smaller than the normal chromosome *III*. The remaining 17 clones were found to be hemizygous for the wild-type allele of locus *III*-205, which suggested that the DNA segment, including locus *III*-205 and locus *III*-314, was absent from their aberrant chromosomes. Because of the variety of sizes, it seemed very likely that the aberrant chromosomes resulted from rejoining of the chromosome *III* at a site somewhere between *III*-205 and its centromere to a site in a chromosome other than the chromosome *III*.

Chromosome loss linked to allelic recombination: As described above, in the 5-FOA^r Leu$^+$ Ade$^-$ convertants, we detected class A clones that were monosomic for chromosome *III* (Table 6B). If the whole chromosome *III* carrying the *URA3* marker was simply lost, the resulting cells would lose the other two markers on the chromosome simultaneously (Figure 5A). In fact, when we isolated and examined 40 clones of 5-FOA^r Leu$^-$ convertants, all of the clones showed the Ade$^-$ phenotype and were monosomic for chromosome *III*. To investigate how the monosomic cells maintaining the Leu$^+$ phenotype were generated, we examined 5-FOA^r Leu$^+$ Ade$^-$ class A clones for their status of the *LEU2* locus by PCR. In this PCR analysis, it is possible to discriminate between wild-type *LEU2* and *leu2Δ1* alleles because the latter allele has a deletion of ∼500 bp. Only the PCR product that corresponded to *leu2Δ1* was detected with 5-FOA^r Leu$^-$ Ade$^-$ class A clones, as expected. On the other hand, with all of the seven 5-FOA^r Leu$^+$ Ade$^-$ monosomics, only a PCR product that corresponded to *LEU2* was amplified. This implied that the *leu2Δ1* allele was absent from these clones. The status of *III*-205 and *III*-314 loci also was examined by PCR, and it appeared that both of the loci were hemizygous for the wild-type alleles in all 5-FOA^r Leu$^+$ Ade$^-$ monosomic clones. These results suggested that the remaining chromosome *III* in these clones consisted of two parts from each homologous chromosome *III*, that is, the left arm portion with *LEU2* from the chromosome *III* that carried all three markers and the right arm portion with the wild-type alleles of *III*-205 and *III*-314 loci from the other chromosome *III*. It seemed probable that the resulting chromosome *III* was generated by allelic crossing over

TABLE 7

Genetic alterations leading to loss of the hemizygous *URA3* marker on chromosome *III*

Classes	Frequency[a] ($\times 10^5$)	Ratio (%)
Loss of chromosome *III*	6.8	55
Interchromosal recombination		
Allelic crossing over	4.3	37
(with loss of chromosome *III*)	0.25	2.1
Gene conversion	0.032	0.27
Ectopic crossing over	0.63	5.5
Intrachromosomal deletion		
(*MAT-HMR* deletion)	0.31	2.6
Intragenic point mutation	0.0071	0.060
Total	12	100

[a] The frequency of each class was estimated by multiplying the frequency of 5-FOA^r Leu$^-$ cells (6.8×10^{-5}), 5-FOA^r Leu$^+$ Ade$^-$ cells (4.9×10^{-5}), and 5-FOA^r Leu$^+$ Ade$^+$ cells (0.35×10^{-5}) by the corresponding ratio of the examined clones of each phenotype, respectively, as explained in the text.

in the interval from *LEU2* to *III*-205 locus. Thus, 5-FOA^r Leu$^+$ Ade$^-$ class A clones were likely to result from such a crossing-over event followed by loss of the chromosome carrying the *URA3* and *ADE2* markers. The frequency of these clones was estimated to be 2.5×10^{-6} whereas the frequency of LOH clones caused by crossing over and that by chromosome loss were 4.0×10^{-5} and 6.8×10^{-5}, respectively (Tables 5 and 6B). Therefore, the Leu$^+$ monosomic clones were unlikely to result from the independent double events of crossing over and chromosome loss taking place sequentially in the population. Rather, the chromosome loss seemed to have occurred in a manner linked to the crossing-over event.

DISCUSSION

In this study we analyzed the physical structure of chromosomes in LOH$^+$ clones that led to functional inactivation of the hemizygous or heterozygous *URA3* marker placed on either chromosome *III* or *V*. The nature of chromosome rearrangements as well as other genetic events leading to the inactivation of the *URA3* marker on chromosome *III* are summarized in Table 7. Spontaneous processes leading to LOH in yeast cells involve mainly three kinds of chromosome alterations, namely, chromosome loss, recombination between allelic loci, and gross rearrangement that generates aberrant chromosomes. Chromosome rearrangement can be further classified into two distinct types of ectopic recombination: intrachromosomal deletion and ectopic crossing over between chromosomes. Although both types of rearrangement were rare, their frequencies were much higher than that of spontaneous point mutation that inactivated the *URA3* marker.

Chromosome loss: Simple loss of chromosome *III* was

the most frequent cause of LOH when the *URA3* marker was located at *III*-205 locus, but was 50-fold less frequent when the authentic *URA3* was present on chromosome *V* (Tables 3 and 7). Previously, frequencies of loss of chromosomes *III* and *V* have been reported to be in the order of 10^{-4} (Campbell *et al.* 1975; Surosky and Tye 1985; Surosky *et al.* 1986; Runge *et al.* 1991) and 10^{-7} to 10^{-5} (Hartwell and Smith 1985; Meeks-Wagner and Hartwell 1986; Santos-Rosa and Aguilera 1994), respectively. Our results are consistent with these estimates and indicate that the frequency of chromosome loss is chromosome specific. Similar chromosome-dependent differences in chromosome loss also have been reported (Malone *et al.* 1980; Esposito *et al.* 1982; Meeks-Wagner and Hartwell 1986; Santos-Rosa and Aguilera 1994; Bruschi *et al.* 1995).

We have provided evidence for a link between chromosome loss and recombination processes. First, the degree of heterogeneity in the *III*-205 locus affected the frequencies of chromosome loss and allelic recombination (Table 3). In the *URA3*-hemizygous strain RD101, ~1.2 kb of discontinuity at *III*-205 is left. Chromosome loss was 2.4-fold more frequent in this strain than the *URA3*-heterozygous strain RD104 while allelic recombination occurred slightly less frequently in RD101 than RD104. Second, several cases of aberrant chromosomes were observed together with loss of another chromosome *III* in the third subtype of class C 5-FOA^r convertants from RD101 (Figure 1; Table 4). Finally, we identified chromosome loss accompanied with allelic recombination events in the 5-FOA^r Leu$^+$ Ade$^-$ isolates from RD301 (Table 6B). Similar observations were reported in previous studies using haploid cells carrying disomic chromosome *III* (Campbell *et al.* 1975; Campbell and Fogel 1977) or *VII* (Esposito *et al.* 1982). Campbell *et al.* suggested that the frequency of recombination could be increased under conditions enhancing chromosome loss. Alternatively, recombination itself might lead to the process involved in the loss of chromosomes. From the ratio between the frequency of chromosome loss accompanied with allelic recombination and that of total events of allelic recombination (Table 7), ~7% of recombination between homologous chromosomes is expected to result in the loss of one of the chromosomes. This could be an overestimate, as our sample size of Leu$^+$ monosomics was too small to accurately determine its frequency (Table 6B). These results, however, suggest that a significant portion of recombination events occurs in a nonconservative fashion and contributes to cause chromosome loss.

Allelic recombination: In class B clones, the *URA3* marker was replaced by the allelic sequence and became homozygous for the locus on either chromosome *III* or *V*. This homogenotization process resulting in LOH might be due to several mechanisms, including crossing over, local gene conversion, and chromosome loss followed by reduplication. Analysis of the *MAT* locus

showed that either gene conversion localized around the *III*-205 locus or allelic crossing over in the interval between *III*-205 and *MAT* loci was responsible for LOH in at least 18% of RD101 class B clones. From the results obtained with RD301, we demonstrated clearly that LOH of class B clones was exclusively due to allelic crossing over in the interval between *CEN III* and *III*-205 (Table 7). Chromosome loss with reduplication did not occur at a detectable level.

Aberrant chromosomes: Analyses with the *III*-205::*URA3*-hemizygous strains (RD101 and RD301) showed that 8% of all LOH$^+$ clones had acquired an aberrant chromosome and that gross rearrangement of chromosomes was largely responsible for this (Tables 3 and 7). The rearrangement was composed of two distinct types of ectopic recombination: intrachromosomal deletion and ectopic crossing over between chromosomes. About one-third of them were intrachromosomal deletions between *MAT* and *HMR* while the remainder were various kinds of interchromosomal rearrangements.

While in haploid yeast strains, chromosome rearrangement, including illegitimate or nonhomologous recombination, has been observed at frequencies similar to or lower than that of point mutation, the occurrence of such spontaneous chromosome aberrations in diploid yeast cells has not been reported previously. Some of the aberrant chromosomes identified here are likely to be produced by unequal crossing over between homologous chromosomes, which means that some genetic methods cannot distinguish LOH$^+$ clones, with this kind of aberrant chromosome, from those caused by allelic crossing over. We found that the occurrence of chromosome aberration was extremely dependent on where the reporter marker was located in the yeast genome (Table 3). When the *URA3* marker was located in the left arm of chromosome *V*, aberrant chromosomes could not be detected in 152 LOH$^+$ clones, which indicated that these aberrations occurred at least 21 times less frequently than in the RD104 strain, where the heterozygous *URA3* marker is situated in the middle of the right arm of chromosome *III*. Therefore, it is difficult to estimate an average frequency of chromosome rearrangement in general.

Intrachromosomal rearrangements: We have shown that chromosome aberration caused by intrachromosomal rearrangements was predominantly a deletion between the *MAT* and *HMR* loci. No other kinds of intrachromosomal deletions were detected in our analysis. This suggests that intrachromosomal deletions, except for the one we identified, occur rarely, at a frequency lower than 3×10^{-8}, which is the minimum detectable level in our analysis. Intrachromosomal deletions have been reported to occur between direct repeats (Lieb-man *et al.* 1979; Rothstein 1979; Roeder and Fink 1982; Winston *et al.* 1984; Downs *et al.* 1985; Christ-man *et al.* 1988; Kupiec and Petes 1988; Boeke 1991; Keil and McWilliams 1993; Klein 1995). These dele-

tions were mostly studied with haploid cells and varied in frequency from 10^{-3} to 10^{-7} and depended on the length of the repeat and the distance between the repeats. About 330 bp of the *LTR* of retrotransposable elements are well-known targets of such intrachromosomal deletions up to 20 kb. According to the SGD database, there exist more than 10 pairs of directly repeated *LTR* sequences, spread over 120 kb across the *URA3* marker on the right arm of chromosome *III*. In our analysis, however, none of the gross deletions between these *LTR* sequences were recovered from more than 10^8 cells while the frequency of Hawthorne deletion was 3.1×10^{-6}. Although the 1.6-kb homologous region between *MAT*a and *HMR* is 4.5 times longer than the 330-bp *LTR* sequences, effects of such differences in the repeat length are known to be less than 10-fold (Yuan and Keil 1990; Jinks-Robertson *et al.* 1993). The distance between the repeated elements also has been shown to affect the occurrence of intrachromosomal gene conversion in *S. cerevisiae*; the proximate repeats undergo gene conversion efficiently over more distant repeats (Roeder *et al.* 1984). The distance between the *LTR* repeats we are studying on chromosome *III* is at least 120 kb, which is much longer than the distance between *LTR* repeats shown to cause intrachromosomal deletions (Liebman *et al.* 1979; Rothstein 1979; Roeder and Fink 1982; Winston *et al.* 1984; Downs *et al.* 1985; Kupiec and Petes 1988; Boeke 1991). These results might imply that the process generating gross deletion requires additional factors other than sequence homology, such as the relative positions of the target sites or the local context of sequences as suggested for the interaction between *MAT* and *HMR* (Wu and Haber 1995; Wu *et al.* 1996; Szeto *et al.* 1997). If this were the case, the type of intrachromosomal deletion we identified in this study would be specific for chromosome *III*.

LITERATURE CITED

Alani, E., L. Cao and N. Kleckner, 1987 A method for gene disruption that allows repeated use of *URA3* selection in the construction of multiply disrupted yeast strains. Genetics **116:** 541–545.

Ausubel, F. M., R. Brent, R. E. Kingston, D. D. Moore, J. G. Seidman *et al.*, 1994 *Current Protocols in Molecular Biology.* John Wiley & Sons, New York.

Baudat, F., and A. Nicolas, 1997 Clustering of meiotic double-strand breaks on yeast chromosome *III*. Proc. Natl. Acad. Sci. USA **94:** 5213–5218.

Boeke, J. D., 1991 Yeast transposable elements, pp. 193–261 in *The Molecular Biology of the Yeast Saccharomyces: Genome Dynamics, Protein Synthesis, and Energetics,* edited by J. R. Broach, J. R. Pringle and E. W. Jones. Cold Spring Harbor Laboratory Press, Cold Spring Harbor, NY.

Boeke, J. D., F. Lacroute and G. R. Fink, 1984 A positive selection for mutants lacking orotidine-5′-phosphate decarboxylase activity in yeast: 5-fluoro-orotic acid resistance. Mol. Gen. Genet. **197:** 345–346.

Bruschi, C. V., J. N. McMillan, M. Coglievina and M. S. Esposito, 1995 The genomic instability of yeast *cdc6-1/cdc6-1* mutants involves chromosome structure and recombination. Mol. Gen. Genet. **249:** 8–18.

Campbell, D. A., and S. Fogel, 1977 Association of chromosome loss with centromere-adjacent mitotic recombination in a yeast disomic haploid. Genetics **85:** 573–585.

Campbell, D. A., S. Fogel and K. Lusnak, 1975 Mitotic chromosome loss in a disomic haploid of *Saccharomyces cerevisiae*. Genetics **79:** 383–396.

Campbell, J. L., and C. S. Newlon, 1991 Chromosomal DNA replication, pp. 48–52 in *The Molecular and Cellular Biology of the Yeast Saccharomyces: Genome Dynamics, Protein Synthesis, and Energetics,* edited by J. R. Broach, J. R. Pringle and E. W. Jones. Cold Spring Harbor Laboratory Press, Cold Spring Harbor, NY.

Carle, G. F., and M. V. Olson, 1987 Orthogonal-field-alternation gel electrophoresis. Methods Enzymol. **155:** 468–482.

Chen, C., and R. D. Kolodner, 1999 Gross chromosomal rearrangements in *Saccharomyces cerevisiae* replication and recombination defective mutants. Nat. Genet. **23:** 81–85.

Chen, C., K. Umezu and R. D. Kolodner, 1998 Chromosomal rearrangements occur in *S. cerevisiae rfa1* mutator mutants due to mutagenic lesions processed by double-strand-break repair. Mol. Cell **2:** 9–22.

Christianson, T. W., R. S. Sikorski, M. Dante, J. H. Shero and P. Hieter, 1992 Multifunctional yeast high-copy-number shuttle vectors. Gene **110:** 119–122.

Christman, M. F., F. S. Dietrich and G. R. Fink, 1988 Mitotic recombination in the rDNA of *S. cerevisiae* is suppressed by the combined action of DNA topoisomerases I and II. Cell **55:** 413–425.

Downs, K. M., G. Brennan and S. W. Liebman, 1985 Deletions extending from a single *Ty1* element in *Saccharomyces cerevisiae*. Mol. Cell. Biol. **5:** 3451–3457.

Drake, J. W., 1991 A constant rate of spontaneous mutation in DNA-based microbes. Proc. Natl. Acad. Sci. USA **88:** 7160–7164.

Esposito, M. S., D. T. Maleas, K. A. Bjornstad and C. V. Bruschi, 1982 Simultaneous detection of changes in chromosome number, gene conversion and intergenic recombination during mitosis of *Saccharomyces cerevisiae* spontaneous and ultraviolet light induced events. Curr. Genet. **6:** 5–11.

Esposito, M. S., R. M. Ramirez and C. V. Bruschi, 1994 Nonrandomly-associated forward mutation and mitotic recombination yield yeast diploids homozygous for recessive mutations. Curr. Genet. **26:** 302–307.

Gedvilaite, A., and K. Sasnauskas, 1994 Control of the expression of the *ADE2* gene of the yeast *Saccharomyces cerevisiae*. Curr. Genet. **25:** 475–479.

Gietz, D., A. St. Jean, R. A. Woods and R. H. Schiestl, 1992 Improved method for high efficiency transformation of intact yeast cells. Nucleic Acids Res. **20:** 1425.

Gupta, P. K., A. Sahota, S. A. Boyadjiev, S. Bye, C. Shao *et al.*, 1997 High frequency in vivo loss of heterozygosity is primarily a consequence of mitotic recombination. Cancer Res. **57:** 1188–1193.

Haber, J. E., D. T. Rogers and J. H. McCusker, 1980 Homothallic conversions of yeast mating-type genes occur by intrachromosomal recombination. Cell **22:** 277–289.

Hartwell, L. H., and D. Smith, 1985 Altered fidelity of mitotic chromosome transmission in cell cycle mutants of *S. cerevisiae*. Genetics **110:** 381–395.

Hawthorne, D. C., 1963 A deletion in yeast and its bearing on the structure of the mating type locus. Genetics **48:** 1727–1729.

Huxley, C., E. D. Green and I. Dunham, 1990 Rapid assessment of *S. cerevisiae* mating type by PCR. Trends Genet. **6:** 236.

Jinks-Robertson, S., M. Michelitch and S. Ramcharan, 1993 Substrate length requirements for efficient mitotic recombination in *Saccharomyces cerevisiae*. Mol. Cell. Biol. **13:** 3937–3950.

Keil, R. L., and A. D. McWilliams, 1993 A gene with specific and global effects on recombination of sequences from tandemly repeated genes in *Saccharomyces cerevisiae*. Genetics **135:** 711–718.

Klein, H. L., 1995 Genetic control of intrachromosomal recombination. Bioessays **17:** 147–159.

Knudson, A. G., 1993 Antioncogenes and human cancer. Proc. Natl. Acad. Sci. USA **90:** 10914–10921.

Kupiec, M., and T. D. Petes, 1988 Allelic and ectopic recombination between *Ty* elements in yeast. Genetics **119:** 549–559.

Lasko, D., W. Cavenee and M. Nordenskjold, 1991 Loss of constitutional heterozygosity in human cancer. Annu. Rev. Genet. **25:** 281–314.

Lea, D. E., and C. A. Coulson, 1948 The distribution of the numbers of mutants in bacterial populations. J. Genet. **49:** 264–284.

Lengauer, C., K. W. Kinzler and B. Vogelstein, 1998 Genetic instabilities in human cancers. Nature **396:** 643–649.

Liebman, S. W., A. Singh and F. Sherman, 1979 A mutator affecting the region of the iso-1-cytochrome c gene in yeast. Genetics **92:** 783–802.

Malone, R. E., J. E. Golin and M. S. Esposito, 1980 Mitotic versus meiotic recombination in *Saccharomyces cerevisiae*. Curr. Genet. **1:** 241–248.

Meeks-Wagner, D., and L. H. Hartwell, 1986 Normal stoichiometry of histone dimer sets is necessary for high fidelity of mitotic chromosome transmission. Cell **44:** 43–52.

Miller, J., 1972 *Experiments in Molecular Genetics.* Cold Spring Harbor Laboratory Press, Cold Spring Harbor, NY.

Newlon, C. S., L. R. Lipchitz, I. Collins, A. Deshpande, R. J. Devenish *et al.*, 1991 Analysis of a circular derivative of *Saccharomyces cerevisiae* chromosome *III*: a physical map and identification and location of *ARS* elements. Genetics **129:** 343–357.

Rivier, D. H., and J. Rine, 1992 An origin of DNA replication and a transcription silencer require a common element. Science **256:** 659–663.

Roeder, G. S., and G. R. Fink, 1982 Movement of yeast transposable elements by gene conversion. Proc. Natl. Acad. Sci. USA **79:** 5621–5625.

Roeder, G. S., M. Smith and E. J. Lambie, 1984 Intrachromosomal movement of genetically marked *Saccharomyces cerevisiae* transposons by gene conversion. Mol. Cell. Biol. **4:** 703–711.

Roman, H., 1956 A system selective for mutations affecting the synthesis of adenine in yeast. C. R. Trav. Lab. Carlsberg Ser. Physiol. **26:** 299–314.

Rose, M. D., F. Winston and P. Hieter, 1990 *Methods in Yeast Genetics: A Laboratory Course Manual.* Cold Spring Harbor Laboratory Press, Cold Spring Harbor, NY.

Rothstein, R., 1979 Deletions of a tyrosine tRNA gene in *S. cerevisiae*. Cell **17:** 185–190.

Runge, K. W., R. J. Wellinger and V. A. Zakian, 1991 Effects of excess centromeres and excess telomeres on chromosome loss rates. Mol. Cell. Biol. **11:** 2919–2928.

Sambrook, J., E. F. Fritsch and T. Maniatis, 1989 *Molecular Cloning: A Laboratory Manual*, Ed. 2. Cold Spring Harbor Laboratory Press, Cold Spring Habor, NY.

Santos-Rosa, H., and A. Aguilera, 1994 Increase in incidence of chromosome instability and non-conservative recombination between repeats in *Saccharomyces cerevisiae hpr1* delta strains. Mol. Gen. Genet. **245:** 224–236.

Schwartz, D. C., and C. R. Cantor, 1984 Separation of yeast chromosome-sized DNAs by pulsed field gradient gel electrophoresis. Cell **37:** 67–75.

Sikorski, R. S., and P. Hieter, 1989 A system of shuttle vectors and yeast host strains designed for efficient manipulation of DNA in *Saccharomyces cerevisiae*. Genetics **122:** 19–27.

Surosky, R. T., and B. K. Tye, 1985 Construction of telocentric chromosomes in *Saccharomyces cerevisiae*. Proc. Natl. Acad. Sci. USA **82:** 2106–2110.

Surosky, R. T., C. S. Newlon and B. K. Tye, 1986 The mitotic stability of deletion derivatives of chromosome *III* in yeast. Proc. Natl. Acad. Sci. USA **83:** 414–418.

Szeto, L., M. K. Fafalios, H. Zhong, A. K. Vershon and J. R. Broach, 1997 Alpha2p controls donor preference during mating type interconversion in yeast by inactivating a recombinational enhancer of chromosome *III*. Genes Dev. **11:** 1899–1911.

Tischfield, J. A., 1997 Loss of heterozygosity or: how I learned to stop worrying and love mitotic recombination. Am. J. Hum. Genet. **61:** 995–999.

Winston, F., D. T. Chaleff, B. Valent and G. R. Fink, 1984 Mutations affecting *Ty*-mediated expression of the *HIS4* gene of *Saccharomyces cerevisiae*. Genetics **107:** 179–197.

Wu, T. C., and M. Lichten, 1994 Meiosis-induced double-strand break sites determined by yeast chromatin structure. Science **263:** 515–518.

Wu, X., and J. E. Haber, 1995 *MAT*a donor preference in yeast mating-type switching: activation of a large chromosomal region for recombination. Genes Dev. **9:** 1922–1932.

Wu, X., J. K. Moore and J. E. Haber, 1996 Mechanism of *MAT alpha* donor preference during mating-type switching of *Saccharomyces cerevisiae*. Mol. Cell. Biol. **16:** 657–668.

Yuan, L. W., and R. L. Keil, 1990 Distance-independence of mitotic intrachromosomal recombination in *Saccharomyces cerevisiae*. Genetics **124:** 263–273.

Zenvirth, D., T. Arbel, A. Sherman, M. Goldway, S. Klein *et al.*, 1992 Multiple sites for double-strand breaks in whole meiotic chromosomes of *Saccharomyces cerevisiae*. EMBO J. **11:** 3441–3447.

Communicating editor: M. Lichten